

Extensive profiling of histidine-containing dipeptides reveals species- and tissue-specific distribution and metabolism in mice, rats, and humans

Citation for published version (APA):

Van der Stede, T., Spaas, J., de Jager, S., De Brandt, J., Hansen, C., Stautemas, J., Vercammen, B., De Baere, S., Croubels, S., Van Assche, C.-H., Pastor, B. C., Vandebosch, M., Van Thienen, R., Verboven, K., Hansen, D., Bove, T., Lapauw, B., Van Praet, C., Decaestecker, K., ... Derave, W. (2023). Extensive profiling of histidine-containing dipeptides reveals species- and tissue-specific distribution and metabolism in mice, rats, and humans. *Acta Physiologica*, 239(1), Article e14020. <https://doi.org/10.1111/apha.14020>

Document status and date:

Published: 01/07/2023

DOI:

[10.1111/apha.14020](https://doi.org/10.1111/apha.14020)

Document Version:

Publisher's PDF, also known as Version of record

Document license:

Taverne

Please check the document version of this publication:

- A submitted manuscript is the version of the article upon submission and before peer-review. There can be important differences between the submitted version and the official published version of record. People interested in the research are advised to contact the author for the final version of the publication, or visit the DOI to the publisher's website.
- The final author version and the galley proof are versions of the publication after peer review.
- The final published version features the final layout of the paper including the volume, issue and page numbers.

[Link to publication](#)

General rights

Copyright and moral rights for the publications made accessible in the public portal are retained by the authors and/or other copyright owners and it is a condition of accessing publications that users recognise and abide by the legal requirements associated with these rights.

- Users may download and print one copy of any publication from the public portal for the purpose of private study or research.
- You may not further distribute the material or use it for any profit-making activity or commercial gain
- You may freely distribute the URL identifying the publication in the public portal.

If the publication is distributed under the terms of Article 25fa of the Dutch Copyright Act, indicated by the "Taverne" license above, please follow below link for the End User Agreement:

www.umlib.nl/taverne-license

Take down policy

If you believe that this document breaches copyright please contact us at:



















repository@maastrichtuniversity.nl

providing details and we will investigate your claim.

Download date: 16 May. 2024

RESEARCH PAPER

Extensive profiling of histidine-containing dipeptides reveals species- and tissue-specific distribution and metabolism in mice, rats, and humans

Thibaux Van der Stede^{1,2}  | Jan Spaas^{1,3,4}  | Sarah de Jager¹  |
 Jana De Brandt^{4,5}  | Camilla Hansen²  | Jan Stautemas¹  | Bjarne Vercammen¹ |
 Siegrid De Baere⁶  | Siska Croubels⁶  | Charles-Henri Van Assche⁷ |
 Berta Cillero Pastor⁷ | Michiel Vandenbosch⁷  | Ruud Van Thienen¹ |
 Kenneth Verboven^{4,5}  | Dominique Hansen^{4,5,8}  | Thierry Bové⁹  |
 Bruno Lapauw¹⁰ | Charles Van Praet^{11,12}  | Karel Decaestecker^{11,12}  |
 Bart Vanaudenaerde¹³ | Bert O. Eijnde^{3,14,15}  | Lasse Gliemann²  |
 Ylva Hellsten²  | Wim Derave¹ 

¹Department of Movement and Sports Sciences, Ghent University, Ghent, Belgium

²Department of Nutrition, Exercise and Sports, Copenhagen University, Copenhagen, Denmark

³University MS Center (UMSC) Hasselt, Pelt, Belgium

⁴BIOMED Biomedical Research Institute, Hasselt University, Diepenbeek, Belgium

⁵REVAL Rehabilitation Research Center, Hasselt University, Hasselt, Belgium

⁶Department of Pathobiology, Pharmacology and Zoological Medicine, Ghent University, Ghent, Belgium

⁷The Maastricht MultiModal Molecular Imaging (M4I) institute, Maastricht University, Maastricht, The Netherlands

⁸Heart Center Hasselt, Jessa Hospital Hasselt, Hasselt, Belgium

⁹Department of Cardiac Surgery, Ghent University Hospital, Ghent, Belgium

¹⁰Department of Endocrinology, Ghent University Hospital, Ghent, Belgium

¹¹Department of Urology, Ghent University Hospital, Ghent, Belgium

¹²Department of Human Structure and Repair, Ghent University, Ghent, Belgium

¹³Department of Chronic Diseases and Metabolism, KU Leuven, Leuven, Belgium

¹⁴SMRC Sports Medical Research Center, BIOMED Biomedical Research Institute, Hasselt University, Diepenbeek, Belgium

¹⁵Division of Sport Science, Stellenbosch University, Stellenbosch, South Africa

Correspondence

Wim Derave, Department of Movement and Sports Sciences, Ghent University, Watersportlaan 2, 9000 Ghent, Belgium.
 Email: wim.derave@ugent.be

Funding information

Research Foundation-Flanders, Grant/Award Number: FWO G080321N, FWO V433222N, FWO 11C0421N, FWO 1138520N and FWO 11B4220N

Abstract

Aim: Histidine-containing dipeptides (HCDs) are pleiotropic homeostatic molecules with potent antioxidative and carbonyl quenching properties linked to various inflammatory, metabolic, and neurological diseases, as well as exercise performance. However, the distribution and metabolism of HCDs across tissues and species are still unclear.

Thibaux Van der Stede, Jan Spaas and Sarah de Jager have contributed equally.

Methods: Using a sensitive UHPLC–MS/MS approach and an optimized quantification method, we performed a systematic and extensive profiling of HCDs in the mouse, rat, and human body (in $n = 26$, $n = 25$, and $n = 19$ tissues, respectively).

Results: Our data show that tissue HCD levels are uniquely produced by carnosine synthase (CARNS1), an enzyme that was preferentially expressed by fast-twitch skeletal muscle fibres and brain oligodendrocytes. Cardiac HCD levels are remarkably low compared to other excitable tissues. Carnosine is unstable in human plasma, but is preferentially transported within red blood cells in humans but not rodents. The low abundant carnosine analogue N-acetylcarnosine is the most stable plasma HCD, and is enriched in human skeletal muscles. Here, N-acetylcarnosine is continuously secreted into the circulation, which is further induced by acute exercise in a myokine-like fashion.

Conclusion: Collectively, we provide a novel basis to unravel tissue-specific, paracrine, and endocrine roles of HCDs in human health and disease.

KEYWORDS

carnosine, central nervous system, exercise, histidine-containing dipeptides, muscle

1 | INTRODUCTION

Carnosine synthase (CARNS1) is presumably the only enzyme in animals capable of synthesizing an abundant class of endogenous dipeptides. The enzyme links L-histidine to either β -alanine or γ -aminobutyric acid (GABA), respectively, rendering carnosine or homocarnosine. These parent dipeptides and their methylated (anserine and balenine) and acetylated (N-acetylcarnosine) analogues are collectively called the histidine-containing dipeptides (HCDs).

Since the initial discovery in 1900 by Vladimir Gulevich,¹ carnosine and the other HCDs have been linked to various physiological functions, mostly serving to preserve redox status and cellular homeostasis (for a full overview, see Ref. [2]). The most relevant biochemical properties for their functions relate to proton buffering, metal chelation, and antioxidant capacity, which further translates to protection against advanced glycation and lipoxidation end products.^{3,4} The physiological importance of tissue HCD content is underscored by an extensive body of research ranging from enhancement of exercise performance⁵ to treatment of cardiometabolic^{6,7} or neurological diseases⁸ in rodents. Major differences between animal and human HCD metabolism may be present, however, given that high carnosinase (CN1) activity in human, but not rodent, plasma results in rapid degradation of carnosine.^{9,10}

Nevertheless, even more than 120 years after the initial discovery of carnosine and 10 years after the molecular identification of CARNS1,¹¹ there remains a lack

of basic understanding of HCD synthesis, distribution, and metabolism throughout the animal and especially the human body. It is thought that HCDs are primarily expressed in excitable tissues such as skeletal and cardiac muscle and the central nervous system (CNS), but current literature mostly consists of scattered observations focusing on a limited number of tissues or species. Information on cardiac levels is sparse, although HCDs could play an important role in cardiomyocyte homeostasis.¹² Furthermore, there is unclarity regarding the synthesis and physiological role of HCDs in kidney, lung, liver, and other non-excitabile tissues. A first profiling of HCDs in rat tissues from Aldini et al.¹³ did not detect HCDs in non-excitabile tissues, although this and other previous endeavors were potentially limited from lower detection sensitivity compared to the currently available technology. For example, the low abundant HCDs anserine, balenine, and N-acetylcarnosine have never been extensively characterized in animal or human tissues.

Here, we have performed the first systematic profiling of the five main HCDs, combined with determination of CARNS1 expression levels, in the mouse, rat, and human body. Various human tissue samples were collected from live donors, except for postmortem collected brain regions. We uncovered profound differences in HCD distribution and metabolism between tissues and species. For instance, we demonstrate that humans have a unique way of circulating HCDs and releasing it from carnosine-synthesizing tissues such as skeletal muscle.

2 | RESULTS

2.1 | CARNS1 is the unique and rate-limiting enzyme for HCD synthesis

Using whole-body *Carns1*-knockout (KO) mice, we aimed to investigate whether CARNS1 deficiency results in a complete lack of endogenous (homo)carnosine and their derivatives in a variety of tissues, which would imply that CARNS1 is the unique and rate-limiting enzyme for HCD synthesis. CARNS1 was successfully knocked out at the gene (Figure 1A) and protein (100 kDa, Figure 1B) level, thereby also validating our western blot antibody for specifically detecting the CARNS1 protein. As described previously, *Carns1*-KO mice displayed normal growth and survival.¹⁴ The deletion of *Carns1* led to an absence of carnosine and homocarnosine in all investigated tissues (Figure 1C). Similarly, these mice were devoid of the carnosine-derived analogs anserine, balenine, and N-acetylcarnosine (of which only anserine is consistently present in mouse tissues, cfr. infra, Figure 1C).

In addition, tissue from *Carns1*-KO mice was used to optimize our quantitative UHPLC-MS/MS-based detection of HCDs. Concentration levels in muscle and brain were compared using matrix-matched standard calibration curve preparation in *Carns1*-KO tissue matrix (i.e., muscle or brain homogenates) and water (as current standard practice in HCD research). In water, HCD levels were overestimated by ~two to threefold (Figure 1D,E), indicating the importance of utilizing a corresponding blank tissue matrix for HCD quantification. This approach was used for all further analyses in this article (except for human cerebrospinal fluid).

2.2 | HCDs are not excitable tissue-specific metabolites

Using our sensitive UHPLC-MS/MS method, we performed a systematic profiling of HCDs in various tissues of the mouse, rat, and human body (Figure 1F, Table S1). Carnosine was the only HCD present in all studied tissues across the three species. Skeletal muscles contained the largest amounts of HCDs, followed by the CNS, up to the millimolar range. However, not all excitable tissue contained large amounts of HCDs, since unexpectedly low HCD levels were observed in the heart of all three species (50–100 times lower than skeletal muscles). These low HCD levels in cardiac tissue better reflect those measured in non-excitable tissues. Besides skeletal muscle, CNS, heart, kidney, adipose, lung, and liver tissue (presented in Figure 1F), we also found low levels of HCDs in the mouse

and rat stomach wall, gallbladder, pancreas, small intestine, colon, thymus, spleen, and eye (Table S1).

2.3 | CARNS1 content drives fibre type-related differences in HCD content in skeletal muscle

We next aimed to profile the HCD content in skeletal muscle in more detail, with a focus on potential fibre type-specific differences. In mice and rats, we determined the HCD content in soleus (more oxidative, slow-twitch) and extensor digitorum longus (EDL; more glycolytic, fast-twitch) muscles. Our results confirmed previous reports^{15–17} that carnosine and anserine content is higher in EDL muscle (Figure 2A). Also, the homocarnosine content was ~2.5-fold higher in EDL compared to soleus in both mice and rats (Figure 2B). To get more insights if CARNS1 content (i.e., HCD production) is the main driver for the fibre type-related differences, we first explored a publicly available human muscle fibre type-specific RNAseq dataset.¹⁸ These data show a ~twofold higher *CARNS1* mRNA content in type IIa versus type I fibres (Figure 2C). We next determined CARNS1 protein levels in the soleus and EDL muscles from the mice and rats (Figure 2D,E). CARNS1 levels were indeed higher in EDL muscles, with a larger difference between soleus and EDL muscles in mice (6.6-fold) than in rats (1.4-fold). To translate mRNA differences in human muscle to the protein level, we used western blotting on pools of pre-classified type I or type IIa fibres (Figure S1). This revealed a ~twofold higher CARNS1 content in type IIa fibres (Figure 2D,E), consistent with findings at the mRNA level. These results suggest that CARNS1 expression is the main driver regulating the clear fibre type-related differences in HCD content across the three species.

2.4 | Homocarnosine is the dominant HCD in the CNS, except for the olfactory bulb of rodents

Aside from skeletal muscle, HCDs are also highly present in the CNS. By analyzing seven different regions from the mouse, rat, and human CNS, we could confirm that the highest levels of carnosine are found in the olfactory bulb in rodents, reaching concentrations of ~1200 $\mu\text{mol/kg}$ tissue, which is similar to or even higher than skeletal muscle carnosine levels (Figure 3A, Table S1). In contrast, the human olfactory bulb contained approximately 15 times less carnosine (~80 $\mu\text{mol/kg}$). In mice and rats, the olfactory bulb was the only CNS region containing more carnosine than homocarnosine, while in humans, all regions contained more homocarnosine than carnosine. Similar to our findings in

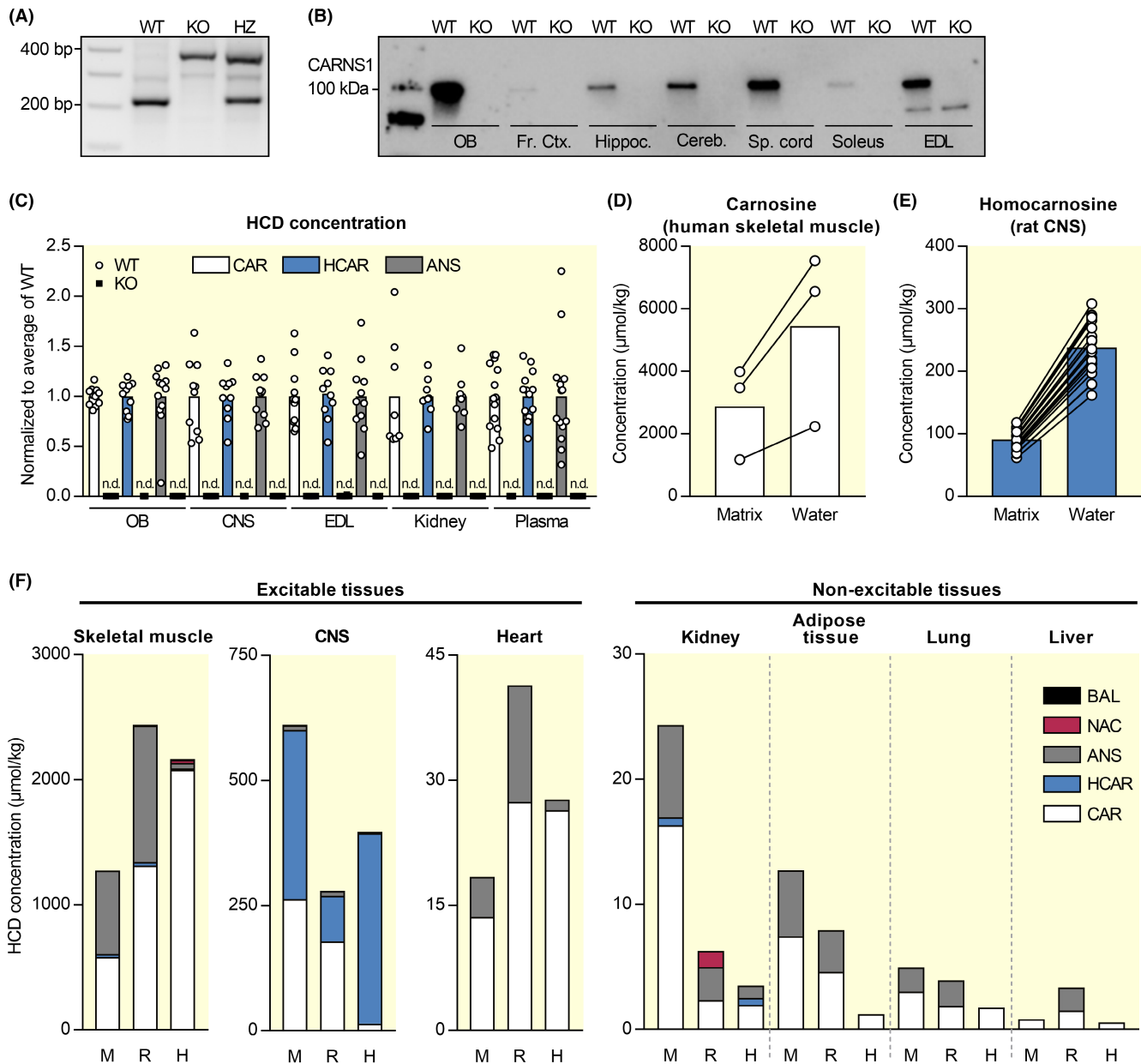


FIGURE 1 Species- and tissue-specific distribution of histidine-containing dipeptides. (A) PCR gel and (B) western blot showing the successful knockout of the *Carns1* gene and the absence of CARNs1 protein in mice. (C) HCD measurements by UHPLC–MS/MS showing HCDs are absent from various tissues of *Carns1*-KO compared to WT mice. (D) Carnosine and (E) homocarnosine measured by UHPLC–MS/MS, followed by quantification based on a standard calibration curve prepared in water versus *Carns1*-KO tissue matrix. (F) HCD measurements by UHPLC–MS/MS in skeletal muscle, CNS, heart, kidney, adipose tissue, lung, and liver tissue from mice (M), rats (R), and humans (H). Values were averaged if more than one type of the respective tissue was present (e.g., soleus and EDL for rodent muscle). ANS, anserine; BAL, balenine; CAR, carnosine; Cereb., cerebellum; CNS, central nervous system; EDL, extensor digitorum longus; Fr. ctx., frontal cortex; HCAR, homocarnosine; Hippoc., hippocampus; HZ, heterozygous; KO, knockout; NAC, N-acetylcarnosine; OB, olfactory bulb; Sp. cord, spinal cord; and WT, wild type.

human CNS tissue, homocarnosine was also abundantly present in human cerebrospinal fluid (Figure 3B). CARNs1 protein levels also showed considerable variability between CNS regions (Figure 3C,D). Mice and rats exhibited high expression in olfactory bulb, as well as the spinal cord and medulla oblongata, but not the rest of the CNS. In human tissues, we found lower CARNs1 levels in the olfactory

bulb, but instead observed greater amounts in the white matter, thalamus, and frontal cortex.

Immunofluorescence was used to further study the localization of CARNs1 in the CNS. We chose the region exhibiting the greatest CARNs1 protein levels among rodents (mouse olfactory bulb) and humans (white matter). Double-labeling of CARNs1 and OLIG2, an oligodendrocyte

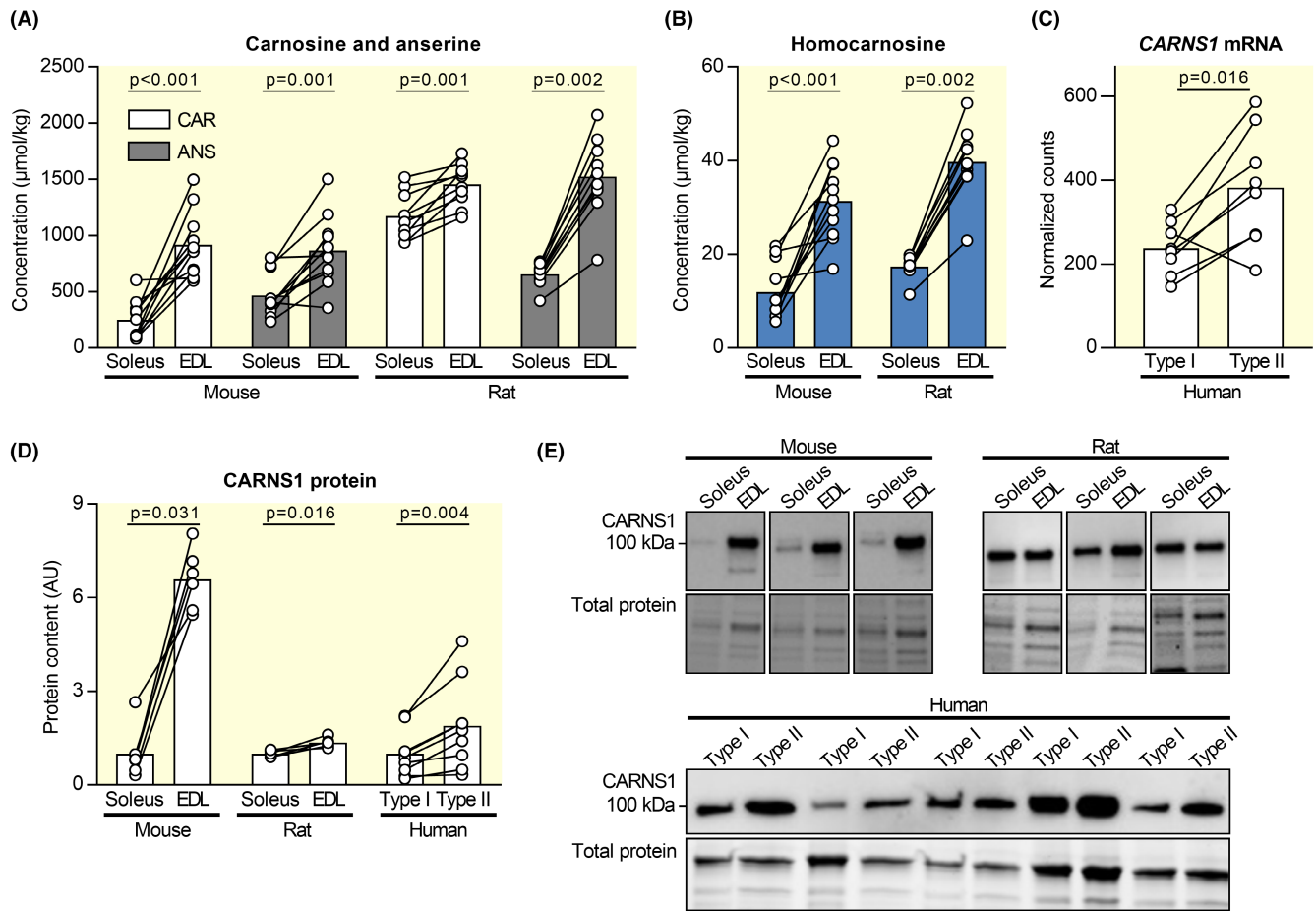
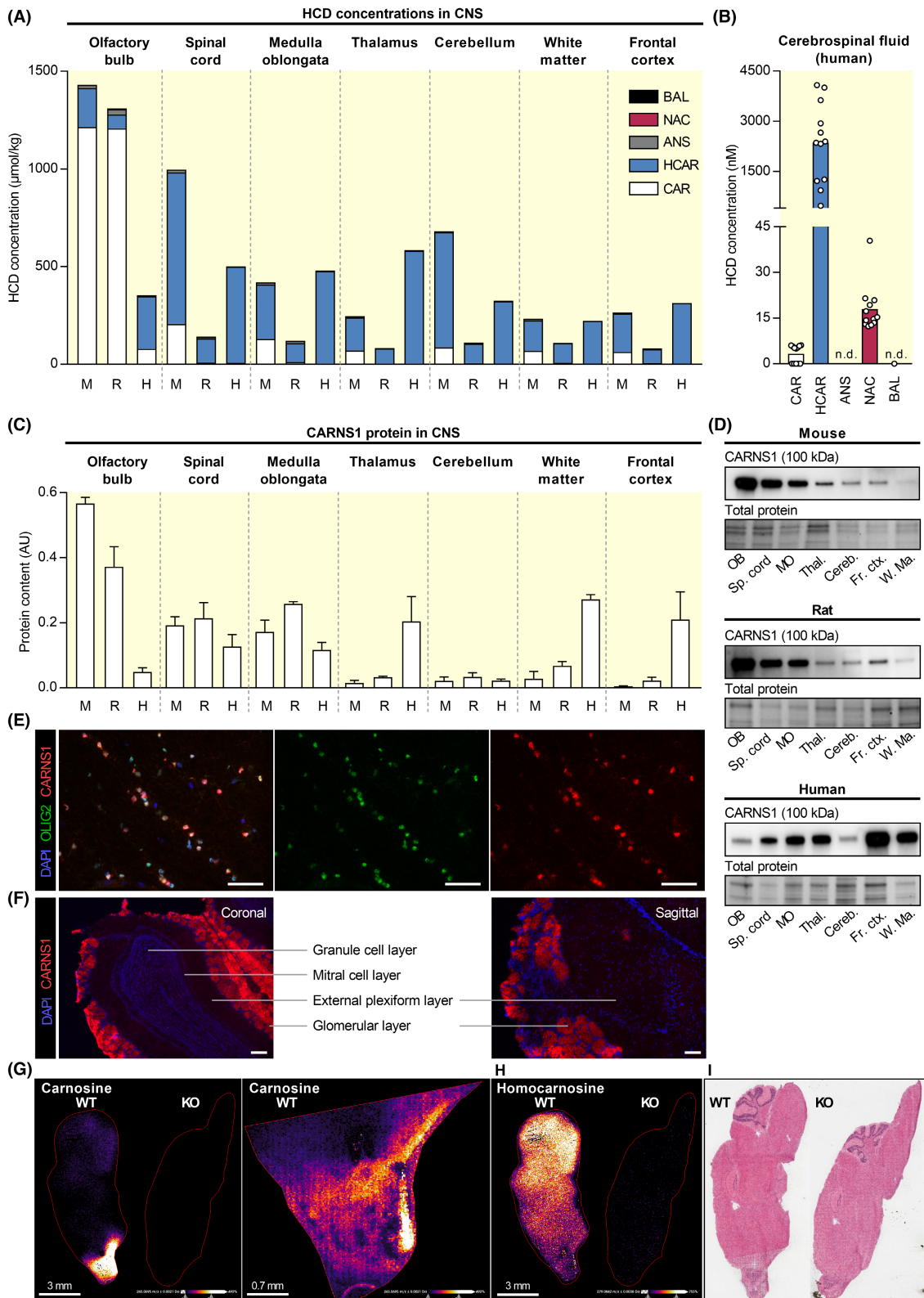


FIGURE 2 Muscle and muscle fiber type-specific differences in histidine-containing dipeptides and CARNS1. (A) Carnosine and anserine and (B) homocarnosine measurements by UHPLC–MS/MS in soleus and EDL muscles from mice and rats. (C) Human muscle fiber type-specific expression of *CARNS1* mRNA based on a previously published dataset. (D) Protein levels of CARNS1 determined by western blot in soleus and EDL muscle from mice and rats, and human type I and type II fiber pools. (E) Representative western blot and loading controls. ANS, anserine; CAR, carnosine; and EDL, extensor digitorum longus.

lineage marker, revealed that CARNS1 resides in oligodendrocytes of human white matter (Figure 3E). Cell markers for microglia (CD68, Figure S2A), astrocytes (GFAP, Figure S2B) and neurons/axons (NF-H, Figure S2C) did not co-localize with CARNS1. In the mouse olfactory bulb, CARNS1 appeared in spherical structures near the surface of the olfactory bulb, that is, the glomeruli, where olfactory nerve terminals form synapses with dendrites from projection neurons that carry signals into the brain (Figure 3F). A similar spatial distribution was present for carnosine, as mass spectrometry imaging detected higher levels at the border compared to the center of the mouse olfactory bulb (Figure 3G). In contrast, homocarnosine displayed a more dispersed distribution throughout the mouse CNS, as well as an overall anterior-to-posterior gradient with greater amounts of homocarnosine in the midbrain, hindbrain, cerebellum, and spinal cord (Figure 3H). As expected, (homo)carnosine could not be detected in *Carns1*-KO mice (Figure 3G–I).

2.5 | CARNS1 expression scales with tissue HCD levels on a whole-body level

To investigate if tissue CARNS1 expression closely relates to tissue HCD levels, CARNS1 protein levels (western blot) were plotted against HCD concentrations (UHPLC–MS/MS). If the tissue CARNS1 level is the main determinant of tissue HCD levels, a linear relation between both variables is expected. In all non-excitatory tissues, no CARNS1 could be detected by western blot (Figure 4A–C). HCD levels in these tissues probably reflect transmembrane HCD uptake. On a whole-body level, CARNS1 scaled with HCD levels in mice (Figure 4A), rats (Figure 4B), and humans (Figure 4C). However, when comparing within organs, more CARNS1 was not always directly linked to a higher HCD concentration. In the human CNS, for example, CARNS1 was 13-fold higher in white matter than in the cerebellum, but both tissues had similar HCD levels.



2.6 | N-acetylcarnosine and balenine are mainly found in human skeletal muscle

While the parent HCDs (carnosine and homocarnosine) were ubiquitously expressed, most of the examined

tissues also contained at least one methylated (anserine or balenine) or acetylated (N-acetylcarnosine) carnosine analog (Figure 1F). Rodent skeletal muscles contained by far the highest anserine levels (up to $\sim 1500 \mu\text{mol/kg}$ in the rat EDL, Figure 5A). Besides

FIGURE 3 Region-specific levels of histidine-containing dipeptides and CARNS1 in the mouse, rat, and human central nervous system. (A) HCD measurements by UHPLC–MS/MS in seven different central nervous system regions from mice (M), rats (R), and humans (H). (B) HCD measurements by UHPLC–MS/MS in human cerebrospinal fluid. (C) Protein levels of CARNS1 determined by western blot in seven different central nervous system regions from mice, rats, and humans. Data are mean \pm SD. (D) Representative western blot and loading controls. (E) Immunohistochemical detection of CARNS1 and OLIG2 in human white matter. (F) Immunohistochemical detection of CARNS1 in mouse olfactory bulb. (G) Mass spectrometry imaging (MALDI-MSI) of carnosine in whole mouse brain (50 μ m spatial resolution) or olfactory bulb only (20 μ m spatial resolution). WT and *Carns1*-KO mouse. (H) Mass spectrometry imaging (MALDI-MSI) of homocarnosine in whole mouse brain (50 μ m spatial resolution). WT and *Carns1*-KO mouse. (I) H&E staining of the representative WT and *Carns1*-KO mouse brains. In panels (A), (C), and (D), spinal cord tissue is from the cervical region, mouse white matter is from the corpus callosum, and human frontal cortex is from the superior frontal gyrus. ANS, anserine; AU, arbitrary units; BAL, balenine; CAR, carnosine; Cereb., cerebellum; CNS, central nervous system; Fr. ctx., frontal cortex; HCAR, homocarnosine; KO, knockout; MO, medulla oblongata; NAC, N-acetylcarnosine; OB, olfactory bulb; Sp. cord, spinal cord; Thal., thalamus; W. Ma., white matter; and WT, wild type. Scale bars are 50 μ m (E), 100 μ m (F).

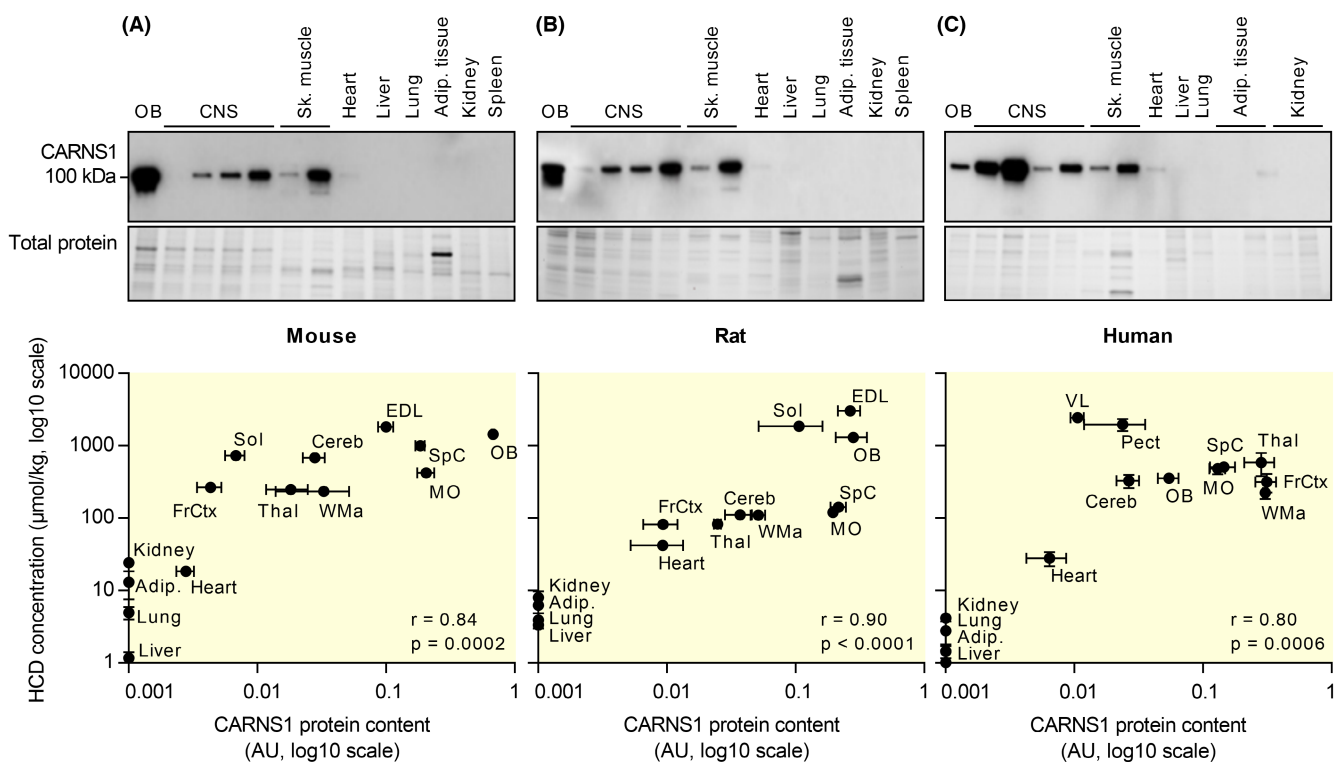


FIGURE 4 Association between CARNS1 and tissue histidine-containing dipeptide levels. Plotted relationship between CARNS1 levels (Western blot) and HCD measurements (UHPLC–MS/MS) in a variety of (A) mouse, (B) rat, and (C) human tissues. The central nervous system (CNS) regions that are shown, besides the olfactory bulb (OB), are frontal cortex (FrCtx), cerebellum (Cereb), spinal cord (SpC), thalamus (Thal), white matter (WMa), and medulla oblongata (MO). Mouse muscles are soleus (Sol) and extensor digitorum longus (EDL). Human muscles are m. vastus lateralis (VL) and m. pectoralis (Pect). Human adipose tissue is subcutaneous and visceral fat (Adip). Human kidney is medulla and cortex. Pearson correlations on log₁₀-transformed data. Data are mean \pm SEM. AU, arbitrary units.

anserine (~40 μ mol/kg, Figure 5A), human skeletal muscle also contained N-acetylcarnosine (~25 μ mol/kg, Figure 5B) and balenine (~5 μ mol/kg, Figure 5C). In fact, human skeletal muscle was the tissue where we observed the highest N-acetylcarnosine and balenine levels. Figure 5D–F display the proportion of methylated or acetylated carnosine variants in different species and tissues.

2.7 | Acetylation of carnosine provides stability in the human circulation, which is not required in red blood cells or rodents

Since rodents and humans differ substantially in presence and activity of the hydrolyzing enzyme CN1 in the circulation,^{2,10} we attempted to map the circulating content of the five main HCDs. As expected, levels of plasma carnosine

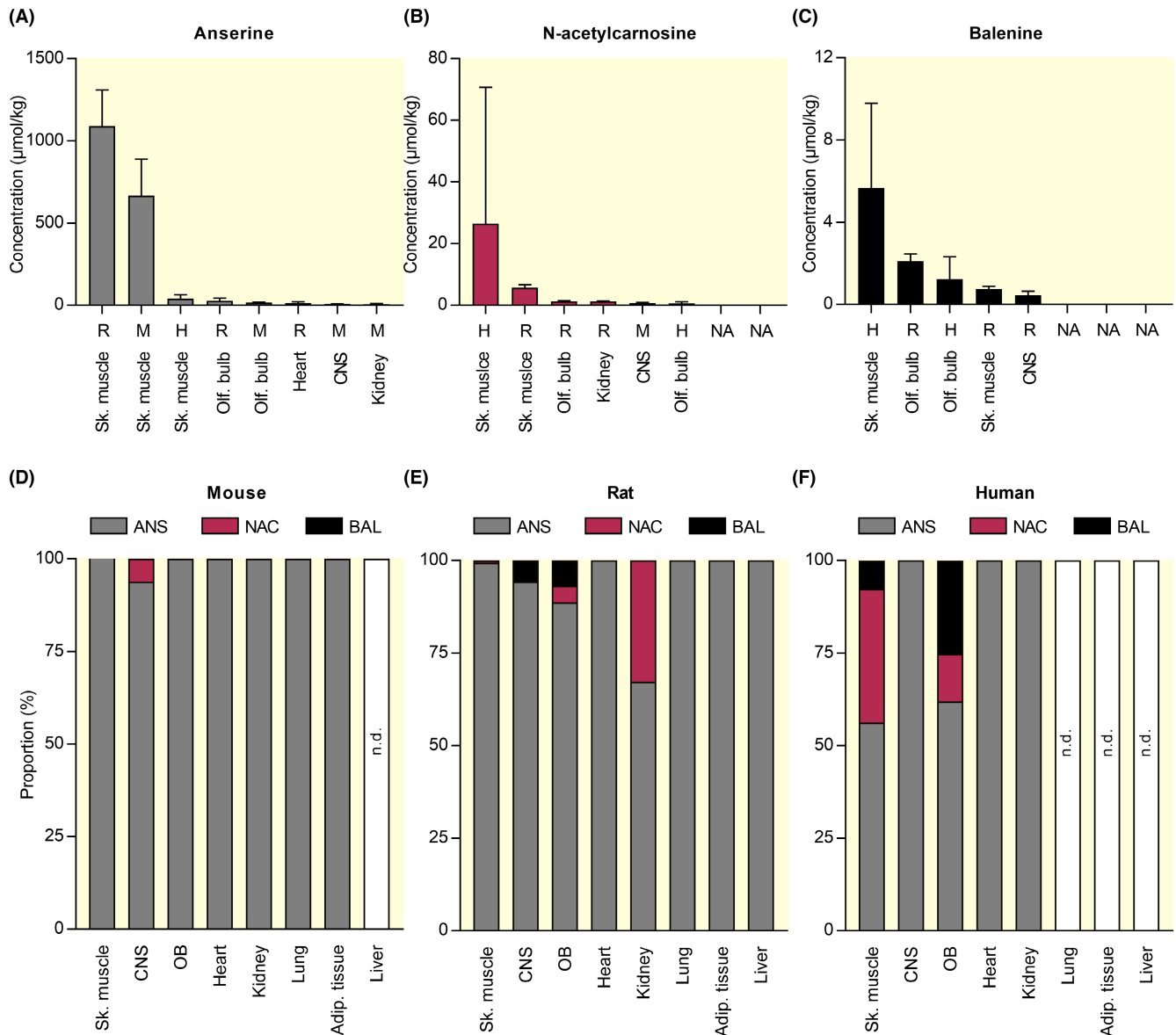


FIGURE 5 Anserine, N-acetylcarnosine, and balenine levels in mouse, rat and human tissues. (A) Anserine, (B) N-acetylcarnosine, and (C) balenine measurements by UHPLC-MS/MS in mouse (M), rat (R), and human (H) tissues. The figures display the eight tissues with the highest concentration of each dipeptide. Data are mean \pm SD. (D-F) Relative proportion of anserine, N-acetylcarnosine, and balenine in (D) mouse, (E) rat, and (F) human tissues. Adip., adipose; ANS, anserine; BAL, balenine; CNS, central nervous system; NAC, N-acetylcarnosine; n.d., not detectable; Olf. bulb, olfactory bulb; and Sk., skeletal.

and anserine were very high in mice (\sim 1500 nM) and rats (\sim 3500 nM), but highly variable and in the low nanomolar range in humans (Figure 6A). Low levels of homocarnosine could be detected in all three species, while balenine was only present in human plasma (Figure 6A). Interestingly, N-acetylcarnosine was the most abundant HCD in the human circulation, accounting for \sim 45% of the total HCDs (Figure 6B). In a subset of the total cohort, we directly compared the HCD levels in plasma versus red blood cells (RBCs) for the three species. Although HCD levels in RBCs were in the nanomolar range in all three species, striking

differences were observed compared to plasma, with the proportion for each HCD being very similar across species (Figure 6C). For both rodent species, HCD levels were drastically lower in RBCs than plasma (Figures 6D and S3). On the contrary, human carnosine and anserine levels were higher in every RBC sample compared to plasma, while N-acetylcarnosine levels were lower in RBCs than plasma (Figure 6E). These data suggest that carnosine in the human circulation is rendered more stable via acetylation to N-acetylcarnosine (which is resistant to hydrolysis by CN1) or via transport inside RBCs.

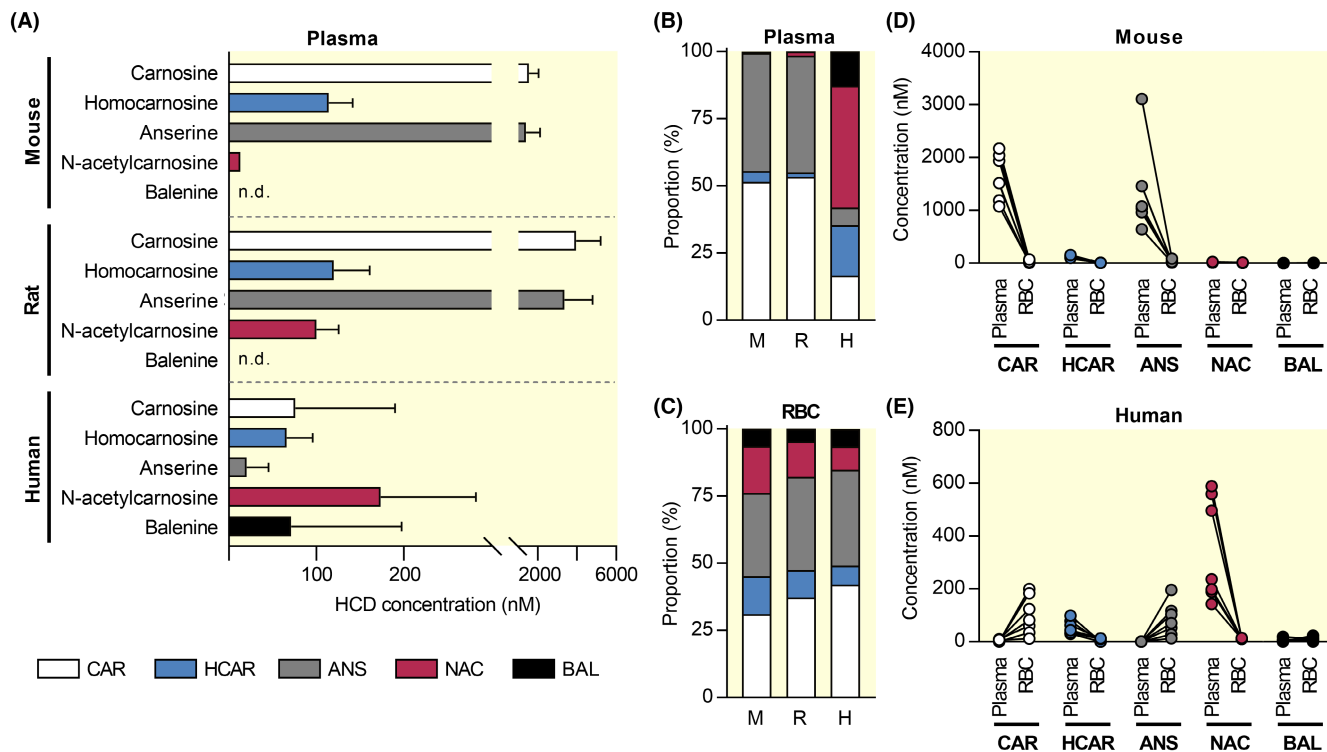


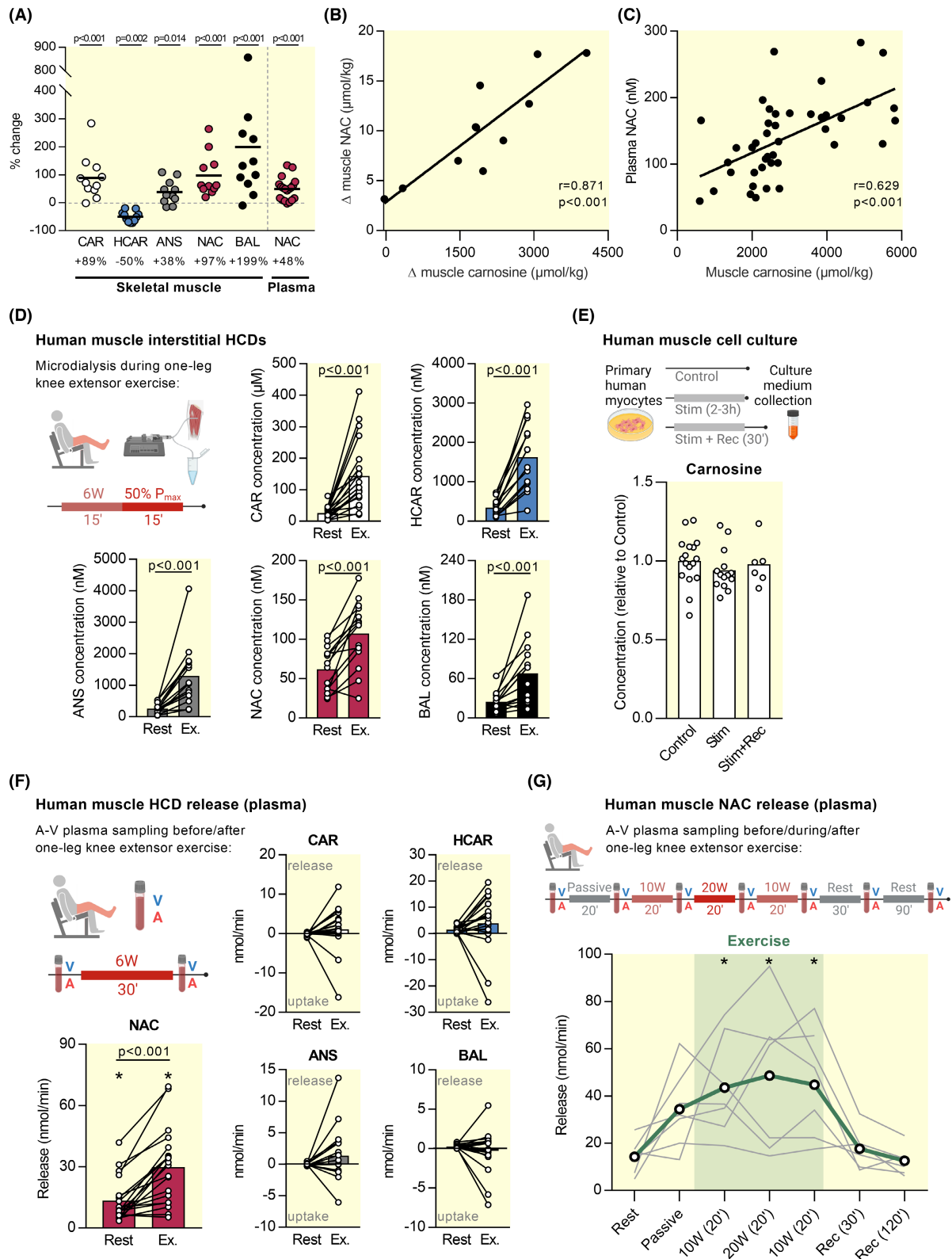
FIGURE 6 Species differences in histidine-containing dipeptides in plasma and red blood cells. (A) HCD measurements by UHPLC-MS/MS in mouse, rat, and human plasma (data are mean \pm SD). (B) Relative proportion of each HCD in mouse (M), rat (R), and human (H) plasma. (C) Relative proportion of each HCD in mouse, rat, and human red blood cells. (D) Direct comparison of HCDs in plasma and red blood cells collected from the same mice. (E) Direct comparison of HCDs in plasma and red blood cells collected from the same human individuals. ANS, anserine; BAL, balenine; CAR, carnosine; HCAR, homocarnosine; NAC, N-acetylcarnosine; and RBC, red blood cells.

2.8 | Oral β -alanine supplementation affects HCDs in skeletal muscle and circulating N-acetylcarnosine levels in humans

We next investigated the effects of chronic supplementation of the rate-limiting precursor β -alanine on the content of all five HCDs in human skeletal muscle. As expected, β -alanine supplementation increased muscle carnosine content (+89%, Figures 7A and S4A). In addition, we observed increases in muscle anserine (+38%, Figures 7A and S4B), N-acetylcarnosine (+97%, Figures 7A and S4C), and balenine (+199%, Figures 7A and S4D), and these increases were proportional to the carnosine increase (Figure 7B). However, homocarnosine content significantly decreased (-50%) after 12 weeks of β -alanine supplementation (Figures 7A and S4E). Plasma N-acetylcarnosine increased by 48% after the supplementation period (Figures 7A and S4F), which correlated at the individual level with muscle carnosine content (Figure 7C), suggesting a possible link between intramuscular and circulating HCD levels. In summary, oral β -alanine supplementation is a potent stimulus affecting all HCDs in skeletal muscle, and plasma N-acetylcarnosine may reflect muscle HCD levels under baseline conditions and during β -alanine supplementation.

2.9 | N-acetylcarnosine is released from human skeletal muscle during exercise

Given this likely relationship between intra- and extracellular HCDs, and given that skeletal muscle is the main active organ during exercise, we explored HCD dynamics during exercise. First, we collected muscle interstitial fluid at rest and during exercise in humans. During exercise, interstitial levels for every HCD increased (Figure 7D). This increase could however be primarily caused by sarcolemmal damage following insertion of the microdialysis probe.¹⁹ To check this, we performed two follow-up experiments. Firstly, *in vitro* human primary muscle cells were electrically stimulated for 2–3 h to simulate muscle contraction. This did not result in secretion of carnosine into the culture medium immediately after the electrical stimulation or following 30 min recovery (Figure 7E). Other HCDs could not be detected in the cell culture medium. Secondly, we collected interstitial fluid from mouse skeletal muscle, with a previously published method in which the muscle is not mechanically affected.^{20,21} Interstitial levels of carnosine and anserine were not higher in exercised mice compared to control mice (Figure S5A). Next, we collected samples of the femoral artery and vein at rest and during exercise (from



a group of postmenopausal women). Our results clearly indicate a release of N-acetylcarnosine from muscle tissue at rest of ~ 13 nmol/min (from one leg), which further increased \sim twofold during exercise (Figure 7F). No release at rest or during exercise was observed for any of the other HCDs (Figure 7F). These results were confirmed using a

similar setup in a separate experiment in healthy young men, and with more sampling time points during rest, passive movement, exercise, and recovery (Figure 7G). Here, we again showed a release of N-acetylcarnosine at rest (~ 14 nmol/min from one leg), which increased 3.4-fold during exercise and quickly returned back to baseline

FIGURE 7 β -alanine supplementation and N-acetylcarnosine release during exercise from human muscle. (A) Changes in HCD levels, measured by UHPLC–MS/MS, in human skeletal muscle (m. vastus lateralis) after β -alanine supplementation. (B) Correlation between supplementation-induced changes in skeletal muscle carnosine and N-acetylcarnosine, measured by UHPLC–MS/MS. (C) Correlation between skeletal muscle carnosine and plasma N-acetylcarnosine, measured by UHPLC–MS/MS. (D) HCD measurements by UHPLC–MS/MS in human skeletal muscle interstitial fluid at rest and following exercise (Ex.). (E) Carnosine measurements by UHPLC–MS/MS in culture medium from primary human muscle cells in control condition, after 2–3 h of electrical stimulation (Stim), and after 2–3 h of electrical stimulation followed by 30 min recovery (Stim+Rec). (F) HCD measurements by UHPLC–MS/MS in human arterial and venous plasma samples at rest and following exercise (Ex.). Positive values indicate a net release, negative values indicate a net uptake. Asterisk indicates significantly different from zero release at the respective time point. (G) Release of N-acetylcarnosine in human plasma, based on arterio-venous differences, at rest, during passive movement, at different time points during exercise, and up to 120 min recovery (Rec). Positive values indicate a net release, negative values indicate a net uptake. ANS, anserine; A-V; arterio-venous, BAL, balenine; CAR, carnosine; HCAR, homocarnosine; and NAC, N-acetylcarnosine.

during recovery (Figure 7G). Exercise did not induce carnosine release or uptake within RBCs (Figure S5B). Also in mice, no changes in carnosine or anserine levels within plasma were observed following 60 min exercise (Figure S5C). Taken together, these data indicate that N-acetylcarnosine in humans is likely the major, or most stable, HCD released during exercise in a myokine-like fashion.

3 | DISCUSSION

This is the first study to systematically and extensively profile the organ distribution of HCDs and their differences between mice, rats, and humans. An overview of the main findings is visualized in Figure 8.

Previous endeavors to profile HCDs mostly focused on rodent tissues, and resulted in fragmented and sometimes contradictory literature.^{13,22–25} Our systematic approach and very sensitive state-of-the-art UHPLC–MS/MS methodology facilitate direct comparison between tissues and species. Our data contradicted some of the previous findings, for example, that human muscle contains only carnosine and no other HCDs,² that rat kidney, lung, plasma, and liver lack HCDs,¹³ or that homocarnosine is exclusively found in the CNS,²⁶ with no presence of carnosine in the human brain or cerebrospinal fluid.²⁷ We confirmed that anserine is predominantly found in rodent skeletal muscles,^{2,16} but add that N-acetylcarnosine and balenine were primarily enriched in human skeletal muscles, although still lower than anserine and (homo)carnosine. From our systematic approach, we calculate that 99.1% of the total amount of HCDs in the human body is found in skeletal muscle tissue, which confirms previous estimations.²⁸ Lower HCD concentrations in skeletal muscle^{29–31} and kidney²³ in our dataset are most likely explained by the use of different (quantification) methods.

CARNS1 and HCDs, especially carnosine, have long been recognized as enriched compounds within the olfactory tract of rodents.^{32,33} Immunostaining and

mass spectrometry imaging revealed the enrichment of CARNS1 and carnosine in the outer (especially glomerular) layers of the mouse olfactory bulb. This also highlights the potential of novel imaging techniques in future HCD research. In human olfactory bulbs, we found remarkably low levels of carnosine compared to homocarnosine. In addition, this is the first study to unequivocally ascribe CARNS1 expression to a specific cell type within the CNS. Our discovery of CARNS1 localization within cells of the oligodendrocyte lineage (human white matter) confirms suggestions from recent RNA sequencing databases of the mouse and human CNS that reported *Carns1*/CARNS1 as an oligodendrocyte-enriched gene within brain parenchyma.^{34,35}

Traditionally, the highest HCD levels are assigned to the excitable tissues. Though this holds true with respect to skeletal muscle and CNS tissue, it was quite compelling that we found extremely low amounts of HCDs in cardiac muscle tissue. In contrast to previous suggestions that the mammalian heart contains ~10 mM total HCDs,^{36,37} we report 100-fold lower levels. The levels of carnosine were more in line with some,^{38,39} but not other^{37,40} studies. Altogether, we thus revoke the hypothesis that N-acetylcarnosine is the dominant HCD in cardiac tissue,¹² which was consistently found in all three species we investigated. It is unclear what causes these low HCD levels in the heart, but a low turnover rate or a role for carnosinase activity are unlikely given the low abundance of CARNS1 and the questionable role of tissue CNBP2 for carnosine homeostasis.^{2,41,42} Nevertheless, HCDs are thought to play a crucial role in cardiac function and recovery from injury.^{12,43} For instance, isolated cardiac myocytes from *Carns1*-transgenic hearts were protected against hypoxia reoxygenation injury,⁴⁴ while *Carns1*-KO rats have impaired cardiac contractility accompanied by reduced Ca^{2+} peaks and slowed Ca^{2+} removal.⁴⁵ This underscores the physiological importance of HCDs and indicates that even low HCD levels can contribute significantly to cell/organ function and health. It remains to be determined, however, which biochemical properties and physiological roles of

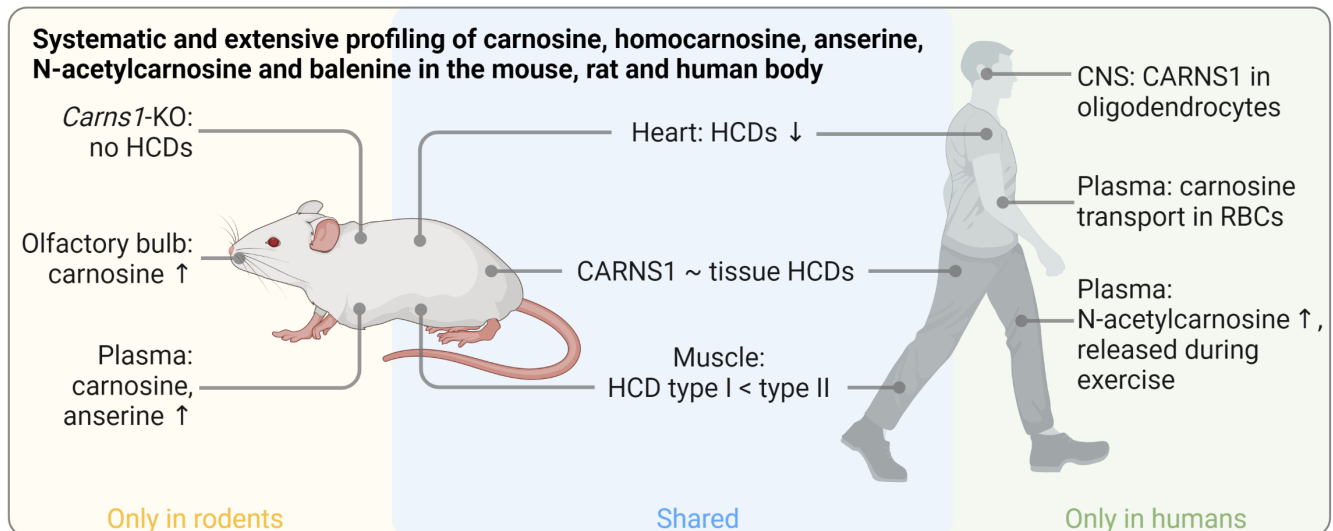


FIGURE 8 Graphical summary. Visual representation of the main findings, based on our extensive profiling of histidine-containing dipeptides (HCDs) in mice, rats, and humans, and related follow-up experiments. 'Arrow up' indicates high abundance; 'arrow down' indicates low abundance. CNS, central nervous system; RBC, red blood cell.

these pleiotropic molecules are the most important in different tissues and under different conditions. With respect to cardiomyocytes, it has been proposed that carnosine functions as a $\text{Ca}^{2+}/\text{H}^{+}$ exchanger to shuttle calcium toward and protons away from the sarcomere site.^{46,47}

The parent HCDs carnosine and homocarnosine share the same synthesizing enzyme CARNS1. This also underlies our observation that oral β -alanine intake leads to increased carnosine but reduced homocarnosine levels in human muscle, suggesting substrate inhibition between GABA and β -alanine for CARNS1 since β -alanine is a 25 times better substrate for CARNS1 than GABA.¹¹ Additionally, high expression of CARNS1 can lead to high tissue content of either carnosine or homocarnosine, probably dependent of the local precursor availability (GABA vs β -alanine). *Carns1*-KO mice did not produce HCDs, whereas in WT mice, rats, and humans, there appears to be a relationship between CARNS1 expression and HCD content on a whole-body level. Moreover, the differences in HCD content between slow- and fast-twitch muscle fibres were paralleled by similar differences in CARNS1 expression. However, the correlation between CARNS1 expression and HCD content was not perfect, suggesting that there might be inter-organ exchange or a role for other HCD-related enzymes such as carnosine N-methyltransferase. An alternative explanation could be a higher HCD turnover in tissues that have an important role for carnosine consumption/recycling, for example, through oxidative stress and reactions with toxic metabolites in pathological conditions.⁸ Alternatively, the fact that CARNS1 shows a preference for β -alanine compared to GABA as a substrate may skew this relationship

considering that some tissues contain more carnosine than homocarnosine and vice versa.¹¹

Tissues that have no or minimal CARNS1 expression likely rely on transmembrane uptake of HCDs derived from exogenous/dietary sources or from production in CARNS1-expressing organs. It has remained unclear, however, if and how HCDs are transported between tissues. The detection of HCDs in various rodent and human tissues likely illustrates that HCDs can be exchanged between organs with and without synthesizing capacity. Indeed, mice that lack the carnosine transporter PEPT2 have altered (mostly reduced) HCD levels in various organs but increased levels in skeletal muscle tissue, which is capable of synthesizing carnosine itself.²² This issue remains largely unclear in humans, in which high activity of the CN1 enzyme quickly degrades circulating carnosine.² It has long been suggested that circulating HCDs are extremely low or absent in human plasma,^{48–50} although more recent reports already detected carnosine.^{51,52} We now demonstrate that N-acetylcarnosine is the most stable carnosine analog in plasma, indicating that acetylation of the β -alanine residue protects against the hydrolyzing activity of CN1, as has been previously suggested.⁵³ Thus, N-acetylcarnosine may be the primary HCD that is exchanged between tissues in humans. Interestingly, plasma N-acetylcarnosine levels were correlated to muscle carnosine (and N-acetylcarnosine) levels, possibly indicating that plasma N-acetylcarnosine can serve as a surrogate marker for intramuscular HCD levels. Plasma N-acetylcarnosine levels increased following β -alanine intake, showing that circulating N-acetylcarnosine levels may also be a marker for muscle carnosine/HCD loading.

In addition, our data indicate that transport of carnosine in RBCs is an alternative strategy to protect against CN1 in human plasma, as recently suggested.^{54,55} This was not true for rodents, who had lower HCD levels in RBCs than humans, despite more than 25 times higher plasma HCD levels.

It has been proposed that carnosine is released from muscles during periods of contractile activity, potentially serving as a health-promoting myokine. This hypothesis is primarily based on a study in rats, where plasma carnosine levels increased during the dark/active phase when animals were provided with a running wheel.⁵⁶ We report that in humans, N-acetylcarnosine is the only HCD that is consistently released from muscle tissue into plasma at rest, which is further increased during periods of muscular activity (exercise), independent of age. This opens various new research avenues on N-acetylcarnosine as an exercise-induced myokine.^{57,58} Future experiments should determine its relevance for exercise training adaptations and cell/organ cross-talk.⁵⁹ The average N-acetylcarnosine release of 14.3 nmol/min from non-contracting leg muscles at rest is striking. Extrapolation of this release to the whole body, assuming that all muscles have the same N-acetylcarnosine secretion, suggests that in theory the blood N-acetylcarnosine concentration should increase by 23.9 μ M every 24 h. Despite this continuous and substantial release of N-acetylcarnosine into the circulation, resting plasma N-acetylcarnosine levels only reach 50–350 nM in most subjects, indicating that there is a large uptake/utilization of N-acetylcarnosine in other organs, or urinary excretion. Based on the amount of N-acetylcarnosine release measured in arterio-venous samples from the leg, we also estimated that a daily turnover of 25% of the total muscle N-acetylcarnosine pool is needed to maintain stable muscle N-acetylcarnosine levels, suggesting a rather dynamic HCD homeostasis in human muscle. Specific description of these calculations and used assumptions can be found in the Supplementary Text. In muscle interstitial fluid samples, all HCDs appear to increase during exercise. However, it is hard to distinguish physiological exercise-induced release from sarcolemmal rupture caused by insertion of the microdialysis probes,¹⁹ as also supported by (I) the lack of other HCD release (besides N-acetylcarnosine) in the venous effluent of contracting muscles, and (II) the absence of a carnosine release during electrical stimulation of primary human muscle cells or interstitial fluid sampled from mice post-exercise. Other physiological stressors, that is, acute and chronic cold challenges, did induce the release of carnosine and anserine from skeletal muscles in mice (A-V measurements).⁶⁰

Despite being the first study to systematically and extensively study the distribution of HCDs in three species,

we acknowledge that the mouse and rat data cannot be fully extrapolated to all mouse and rat strains, since these can differ somewhat.⁶¹ We also decided to focus on the two parent HCDs (carnosine and homocarnosine) and carnosine's methylated and acetylated analogs (anserine, balenine, N-acetylcarnosine). Other HCD conjugates do exist, but these are mostly very low abundant products from reactions with other (toxic) compounds (e.g., carnosine-propanol or 2-oxo-carnosine^{62–64}). Furthermore, follow-up experiments on the functional relevance of the exercise-induced release of N-acetylcarnosine from human skeletal muscle, should be explored in future research.

In conclusion, we extensively profiled the organ distribution of the five main HCDs and discovered new physiological routes of HCD metabolism. Our results can be used to generate various new research hypotheses and highlight that findings derived from animal research on HCDs cannot always be translated to humans. In particular, the apparent inter-cell and inter-tissue para- and endocrine regulation of HCDs in relation to human health, disease, and exercise performance/adaptation, deserves further investigation.

4 | MATERIALS AND METHODS

4.1 | HCD profiling—Rodent tissue collection

All mouse tissues were obtained from an in-house breeding of *Carns1*-KO and WT mice with a C57/BL6 background, kindly provided by Prof. M. Eckhardt.^{14,65} Genotypes of the offspring from heterozygous parents were determined in toe samples using a previously published protocol.¹⁴ Wistar rats were supplied by Envigo (The Netherlands). Mice and rats were housed under standard room conditions (12h:12h light: dark cycle, 20–24°C, relative humidity 30%–60%) and had ad libitum access to drinking water and food pellets. For tissue collection, female and male animals were killed at an age of 6–10 weeks (mice) or 7–8 weeks (rats) old. Following overdose injection of Dolethal (200 mg/kg, i.p.), blood was collected from the right ventricle, kept in Multivette® 600 K3 EDTA vials on ice, centrifuged (5 min, 3500 rpm), and plasma was stored at –80°C. Before tissue dissection, mice and rats were perfused with 0.9% NaCl solution containing heparin (25 UI/mL) via a left ventricular puncture. For determination of HCD levels by UHPLC–MS/MS and CARNS1 expression by western blot, the tissues were immediately frozen in liquid nitrogen, before being stored at –80°C. For immunohistochemistry, whole mouse brains were carefully placed on a metal plate cooled by dry ice in a foam box for several minutes, wrapped in aluminum foil, and stored at –80°C. Mouse exercise experiments were performed on a

treadmill (6 m/min, speed increased every 2 min by 2 m/min until 16 m/min, total duration 60 min), and were preceded by a 1-week adaptation period (three running sessions, gradually increasing exercise intensity and duration). Sedentary mice were placed on a stationary treadmill for 60 min. Immediately after exercise, plasma was obtained and mice were perfused as described above. To collect interstitial fluid, gastrocnemius muscles were placed on 20 μ M nylon net filters (Millipore, cat# NY2004700) and centrifuged (10 min, 800 \times g).^{20,21} All animal procedures were approved by the Ethical Committee on Animal Experiments at Hasselt University (202074B, 202127, and 202145).

4.2 | HCD profiling—Human tissue collection

All human samples were obtained after written informed consent.

4.2.1 | Human vastus lateralis muscle

Muscle biopsies were collected from the m. vastus lateralis of healthy, young volunteers using the Bergström needle biopsy technique with suction, as described previously.⁶⁶ One part of the samples was immediately snap-frozen in liquid nitrogen and stored at -80°C until UHPLC–MS/MS analysis. The other part was submerged in 1–1.5 mL of RNAlater (Thermo Fisher Scientific), stored at 4°C for maximum 48 h and subsequently stored at -80°C for later individual fibre dissection.

4.2.2 | Human heart and pectoralis muscle

Heart and pectoralis muscle samples were collected from patients undergoing open heart surgery under general anesthesia. Heart samples consisted of the right atrial appendage, harvested at the time of venous drainage cannulation for cardiopulmonary bypass. Samples were immediately snap-frozen in liquid nitrogen and stored at -80°C . For Figure 1F, HCD concentrations of vastus lateralis and pectoralis muscle were averaged.

4.2.3 | Human kidney

Kidney samples were collected from patients undergoing radical nephrectomy. In case of kidney cancer, tissue was sampled as far away from the site of the tumor to obtain the healthiest part of the kidney, immediately snap-frozen in liquid nitrogen, and stored at -80°C . Medulla and

cortex were sampled separately (Table S1), but data were later averaged for analysis and visualization.

4.2.4 | Human adipose tissue

Visceral and subcutaneous adipose tissue were sampled from lean and obese individuals during abdominal surgery following an overnight fast.⁶⁷ Tissue pieces were rinsed, freed from visible blood and connective tissue, and snap-frozen in liquid nitrogen. The two subtypes (Table S1) were later averaged for analysis and visualization.

4.2.5 | Human lung

Lung tissue was obtained from unused healthy donor lungs that were not used for transplantation from the BREATH KULeuven biobank (S51577).

4.2.6 | Human liver

Liver samples were surgically removed from fasted subjects with obesity during gastric bypass surgery. Exclusion criteria were the presence of malignancies, drinking more than two units (women) or three units (men) of alcohol per day, having known liver pathologies other than non-alcoholic fatty liver disease. For this analysis, five samples with NAS score 0 or 1 were selected.⁶⁸

4.2.7 | Human plasma and RBC

Blood samples were always collected in pre-cooled EDTA tubes, after a 1–2-day lacto-ovo vegetarian diet to ensure no influence of dietary HCD intake. For plasma, samples were immediately centrifuged (10 min, 3000 \times g, 4°C), followed by immediate deproteinization (110 μ L of 35% 5-sulfosalicylic acid per 1 mL of plasma) and second centrifugation (5 min, 15000 \times g, 4°C). Plasma samples were then stored at -80°C . For RBC isolation,⁶⁹ blood tubes were centrifuged for 15 min at 120 \times g at room temperature. Plasma was carefully removed and 200 μ L RBCs were collected in 1.8 mL of ice-cold methanol (55% v/v). Samples were then stored at -80°C .

4.2.8 | Human CNS

Seven different human CNS regions were obtained from The Netherlands Brain Bank (NBB), Netherlands Institute for Neuroscience, Amsterdam (open access www.brain

bank.nl). All donors were “non-demented controls,” indicating the absence of neurological and psychiatric disease. From two subjects, all seven regions were available. For immunohistochemical analyses, white matter tissue from healthy controls and unaffected white matter tissue of multiple sclerosis patients from a previous study was used.

4.2.9 | Human cerebrospinal fluid

Cerebrospinal fluid from subjects without neurological disease at the time of sampling was obtained via the University Biobank Limburg (UbiLim), with approval from the Medical Ethics Committee at Hasselt University (CME2021-004). Lumbar cerebrospinal fluid was collected into PPS tubes, kept at 4°C, centrifuged to remove cells (10 min, 500 × g, 4°C), and supernatant was stored at -80°C.

4.3 | Human β-alanine supplementation study

Vastus lateralis muscle biopsies obtained via the Bergström needle biopsy technique with suction ($n=11$ β-alanine, $n=11$ placebo) and plasma samples ($n=19$ β-alanine, $n=17$ placebo) were collected before and after 12 weeks of β-alanine supplementation in patients with COPD (sustained-release CarnoSyn®, NAI). Methodological details have been described previously.⁷⁰ Snap-frozen biopsies were freeze-dried for 48 h, followed by manual removal of non-muscle material (fat, connective tissue, and blood) under a light microscope. Effects of β-alanine were analyzed using a two-way repeated measures ANOVA (group vs time) for each HCD separately, followed by Sidak's multiple comparisons tests. Correlations were performed using Pearson correlation (Δ muscle carnosine vs Δ N-acetylcarnosine) or Spearman rank correlation (muscle carnosine vs plasma N-acetylcarnosine).

4.4 | Human HCD release experiments

4.4.1 | Microdialysis experiment

Detailed methodology has been described previously.⁷¹ In short, interstitial samples from m. vastus lateralis were collected using the microdialysis technique at rest and after 30 min of one-legged knee extensor exercise (15 min 6 W, 15 min 50% peak power). Subjects consisted of a group of young ($n=7$) and old ($n=13$) healthy men

(results are pooled together since no differences between groups could be observed). Concentrations were corrected for probe recovery as determined by relative loss of [2-3H]-labeled adenosine in the dialysate. Interstitial levels during exercise were compared to resting values using a multiple Wilcoxon matched-pairs signed rank test with Holm-Sidak multiple comparison test.

4.4.2 | Arterio-venous balance experiment 1

Arterial and venous samples were collected from the femoral artery/vein at rest and after 30 min one-legged knee extensor exercise (6 W) in a group of healthy postmenopausal women ($n=19$). Methodological details have been described before.⁷² Samples were deproteinized with 35% 5-sulfosalicylic acid, as described above, on the day of the UHPLC-MS/MS analysis. Exercise versus resting HCD levels were compared using a multiple Wilcoxon matched-pairs signed rank test with Holm-Sidak multiple comparison test.

4.4.3 | Arterio-venous balance experiment 2

Seven healthy, young men (28 ± 4 years old, BMI of 24 ± 2 , VO_{2max} of 49 ± 7 mL/min/kg) participated in this experiment. After passive transport to the laboratory, catheters were inserted in the femoral artery and vein. Next, arterial and venous samples were collected every 30 min during a 90-min supine resting period. After this, 20 min of passive leg movement was performed, followed by 60 min of active one-legged knee extensor exercise (20 min 10 W, 20 min 20 W, and 20 min 10 W). Samples were collected at the end of each exercise bout. Finally, arterio-venous samples were collected after 30 min and 2 h of recovery. Plasma and RBC samples were collected as described above. Exercise-induced effects were analyzed using a mixed-effect model with repeated measurements over time, with post hoc comparison of every time point versus baseline (Holm-Sidak test).

4.5 | Primary cell culture experiments

Biopsy samples (~150 mg) were obtained from m. vastus lateralis from young, healthy men. Primary skeletal muscle cells were isolated with homemade antibody-coated magnetic beads and cultured as previously described.^{73,74} Cultured skeletal muscle cells were used for analysis on day 5 or 6 after the onset of differentiation. At this time, most of the myocytes have differentiated into multinucleated myotubes and can easily

be identified as muscle cells. Myotubes were starved with media containing 0.1% bovine serum albumin (DMEM without phenol, D-glucose, and L-glutamine) for 16 h before experiments. The skeletal muscle cells were electro-stimulated as described previously,⁷⁵ with the minor addition of 5 μM (S)-nitro-Blebbistatin (Cayman Chemical, CAS. 856 925–75-2) to the stimulation buffer to inhibit the spontaneous contraction of the myotubes.⁷⁶ The cells were stimulated for 2–3 h (50 Hz, 0.6 s/0.4 s trains, 1 ms pulse width, and 10 V, homemade electrical stimulator connected to a Digitimer MultiStim SYSTEM-D330). The extracellular medium was collected immediately or 30 min after the end of stimulation, and medium from non-stimulated control cells was harvested simultaneously. Changes over time were analyzed using a mixed-effect model with repeated measurements over time, with post hoc comparison of stimulated and stimulated+recovery versus control cells (Holm–Sidak test).

4.6 | HCD determination by UHPLC–MS/MS

Details of the validation of the in-house developed UHPLC–MS/MS analysis have been described previously,^{77,78} and are presented in Table S2–S6. The limit of detection was determined to be 5–10 nM (in plasma), corresponding to 0.38–0.76 $\mu\text{mol/kg}$ tissue for our homogenization protocol. Pure carnosine and anserine were kindly provided by Flamma S.p.a. (Chignolo d'Isola, Bergamo, Italy), and pure balenine by NNB Nutrition (Frisco, Texas, USA). Homocarnosine (#33695) and N-acetyl-L-carnosine (#18817) were purchased from Cayman Chemical (Ann Arbor, Michigan, USA). UHPLC–MS/MS data extraction and analysis was performed using Masslynx software 4.2 (Waters, Milford, USA).

4.6.1 | Tissues

All tissues were prepared similarly, based on the method described previously.⁸ Frozen tissues were quickly weighed and immediately homogenized in extraction solution (ultrapure water with 10 mM HCl and internal standard carnosine-d4) in a ratio of 95 μL extraction solution per 5 mg tissue in a QIAGEN TissueLyser II (1 min, 30 Hz). The concentration of carnosine-d4 varied according to expected HCD concentrations in the tissues: muscle (20 μM), CNS (5 μM), liver/lung/spleen (0.5 μM), and all other tissues (1 μM). Then, homogenates were centrifuged (20 min, 3000 $\times g$, 4°C). Supernatants were immediately diluted in a

3:1 ratio with ice-cold acetonitrile (–20°C), vortexed, and kept on ice for 15 min. After a second centrifugation step (20 min, 3000 $\times g$, 4°C), samples were stored at –80°C until the day of the UHPLC–MS/MS analysis. Samples were combined with 75:25 acetonitrile: water in a 4:1 ratio before injection in the UHPLC–MS/MS device. For skeletal muscle and CNS, samples were also injected after an extra initial dilution (1:25 for muscle, 1:10 for CNS) for the determination of carnosine (skeletal muscle) and homocarnosine (CNS) content. Standard calibration curves were prepared for each individual run and for each tissue separately in the respective tissue of the *Carns1*-KO mice to account for possible tissue matrix effects (for all three species). Differences between soleus and EDL HCD levels in mice and rats were analyzed using paired t-tests or Wilcoxon signed rank tests, depending on normality of the data.

4.6.2 | Plasma

Deproteinized plasma (150 μL) was combined with acetonitrile containing 1% formic acid (215 μL), 1 μM carnosine-d4 as internal standard (10 μL), and ultrapure water (25 μL). For mouse plasma analysis, volumes were scaled down to available plasma (75 μL). After thoroughly vortexing, samples were centrifuged (15 min, 15000 $\times g$, 4°C). The supernatant was collected and injected in the UHPLC–MS/MS. A standard calibration curve was prepared in a pool of human deproteinized plasma that was collected after a 2-day lacto-ovo vegetarian diet to minimize circulating HCDs (for all three species).

4.6.3 | RBC

First, 190 μL of the RBC samples was combined with 10 μL of internal standard carnosine-d4 (2 μM) and 10 μL of 75:25 acetonitrile: water (with 1% formic acid). This mixture was vortexed and then centrifuged in a 10 kDa filter (Nanosep® Centrifugal Device with Omega Membrane™, Pall Corporation). The supernatant was subsequently evaporated at 40°C and the droplet resuspended in 40 μL of 75:25 acetonitrile: water (with 1% formic acid) before injection in the UHPLC–MS/MS device. A standard calibration curve was prepared in a pool of human RBC samples that were collected after a 2-day lacto-ovo vegetarian diet to minimize circulating HCDs (for all three species).

4.6.4 | Cerebrospinal fluid

Human cerebrospinal fluid was treated identically as plasma, but the standard calibration curve was prepared

in ultrapure water since no *Carns1*-KO tissue matrix was available, possibly resulting in overestimation of the absolute concentrations.

4.6.5 | Interstitial fluid

Interstitial fluid (15 μ L) was combined with 30 μ L acetonitrile containing 1% formic acid and 1 μ M carnosine-d4 and 10 μ L ultrapure water. This mixture was vortexed, centrifuged (15 min, 15 000 \times g, 4°C), and the supernatant was used to inject in the UHPLC-MS/MS. For detection of carnosine in humans, samples were first diluted 1:30. For detection of carnosine and anserine in mice, samples were first diluted 1:500. A standard calibration curve was prepared in Ringer-Acetate buffer as this was used to perfuse the microdialysis probes.

4.6.6 | Cell culture medium

Extracellular medium (150 μ L) was mixed with acetonitrile containing 1% formic acid (240 μ L) and internal standard carnosine-d4 (2 μ M, 10 μ L), vortexed, and injected in the UHPLC-MS/MS. A standard calibration curve was prepared in DMEM culture medium.

4.7 | CARNS1 protein levels by western blot

Tissues were diluted in RIPA buffer (300 μ L per 10 mg tissue; 50 mM Tris pH 8.0, 150 mM NaCl, 0.5% sodium deoxycholate, 0.1% SDS, 1% Triton-X100, and freshly added protease/phosphatase inhibitors [Roche]), and homogenized using stainless steel beads and a QIAGEN TissueLyser II (shaking 1 min, 30 Hz). Following centrifugation (15 min, 12 000 \times g, 4°C), supernatants were stored at -80°C. Pierce™ BCA Protein Assay Kit (Thermo Fisher) was used according to manufacturer's instructions to determine protein concentrations (read at 570 nm wavelength). For detection of CARNS1 protein levels, 1 μ g of protein was diluted in loading buffer solution (63 mM Tris Base pH 6.8, 2% SDS, 10% glycerol, 0.004% Bromophenol Blue, and 0.1 M DTT), heated for 4 min at 95°C, and separated in polyacrylamide gels (4–15%, Mini-PROTEAN TGX, Bio-Rad) at 100–140 V on ice. Next, stain-free gels were imaged following UV exposure to visualize total protein content (ChemiDoc MP Imaging System, Bio-Rad). Proteins were transferred from the gel to an ethanol-immersed PVDF membrane in transfer buffer (30 min, 25 V, 1.0 A, Trans-Blot Turbo Transfer System, Bio-Rad). Membranes were briefly washed in Tris-buffered saline

with 0.1% Tween20 (TBS-T), and blocked for 30 min using 3% milk powder in TBS-T. Following overnight incubation at 4°C with primary antibodies against CARNS1 (rabbit polyclonal, 1:1000 in 3% milk/TBS-T, HPA038569, Sigma), membranes were washed (3 \times 5 min), incubated with secondary HRP-conjugated goat anti-rabbit antibodies (1:5000 in 3% milk/TBS-T) for 60 min at room temperature, washed again (3 \times 5 min), and chemiluminescent images were developed in a ChemiDoc MP Imaging System (Bio-Rad) using Clarity Western ECL substrate (Bio-Rad). CARNS1 protein bands were quantified with Image Lab 6.1 software (Bio-Rad), and normalized to total protein content from the stain-free image. Finally, bands were expressed relative to total CARNS1 expression (sum of all bands) of a particular mouse, rat, or human. For muscle, band densities were expressed as fold changes relative to the average density from soleus muscles per blot. Linearity of the signal was determined for every tissue. Differences between soleus and extensor digitorum longus CARNS1 content were analyzed using a paired t-test (rat) or Wilcoxon signed rank test (mouse), depending on normality of the data. Pearson correlations on log10-transformed data were used to scale CARNS1 proteins levels to tissue HCD content.

4.8 | CARNS1 protein level in human single muscle fibres

CARNS1 protein levels in type I versus type II muscle fibres were determined based on a previously published method.⁷⁹ Muscle samples in RNAlater (Thermo Fisher Scientific) were thawed and subsequently transferred to a petri dish filled with fresh RNAlater (Thermo Fisher Scientific) solution. Individual muscle fibres were manually dissected under a light microscope and immediately submerged in a new 0.5 mL tube with 5 μ L ice-cold Laemmli buffer (125 mM Tris-HCl (pH 6.8), 10% glycerol, 125 mM SDS, 200 mM DTT, and 0.004% bromophenol blue). Tubes were then incubated for 15 min at 4°C, followed by 10 min at 70°C, and then stored at -80°C until the next step of the analysis. A total of 40–72 fibres were isolated from nine biopsies. Next, muscle fibre type (based on myosin heavy chain expression) was determined using dot blotting techniques. For this, 0.5 μ L of the muscle fibre lysate was spotted onto two activated and equilibrated PVDF membranes, one for MHC I and one for MHC IIa. After air-drying the PVDF membrane for 30 min, it was re-activated in 96% ethanol and equilibrated in transfer buffer (8 mM Tris-base, 39 mM glycine, 0.015% SDS, and 20% ethanol). The next steps are similar to standard western blotting as described above, with primary antibodies for MHC I (A4.840, 1:1000 in 3% milk in TBS-T, DSHB) or MHC IIa (A4.74, 1:1000 in 3% milk in TBS-T, DSHB). Fibre

lysates were classified as type I or IIa fibres based on a positive stain for only the MHC I or IIa antibody (Figure S1). Next, fibres of the same type from the same subject were pooled ($n=10-26$ for type I and $n=9-22$ for type IIa fibres). CARNS1 protein content in these fibre type-specific samples were determined with standard western blotting technique as described above, with loading of 5 μ L per pool. Band densities were expressed as fold changes relative to the average density from type I fibres per blot. Statistical analysis was performed using a Wilcoxon signed rank test.

4.9 | CARNS1 mRNA expression

The fibre type-specific RNAseq dataset of Rubenstein et al. was downloaded from the GEO repository under accession number GSE130977.¹⁸ This dataset consists of RNAseq data of pools of type I or type II fibres from *m. vastus lateralis* biopsies of nine healthy, older men. For full details on generation of this dataset, we refer to the original publication. Raw counts were normalized with DESeq2 to allow for between-sample comparisons.⁸⁰ First, normalized counts for *MYH2* (ENSG00000125414, type II fibres) and *MYH7* (ENSG00000092054, type I fibres) were extracted and assessed for each fibre pool as purity quality control. Based on this analysis, the fibre pools of one participant were excluded for further analysis. Next, normalized counts of *CARNS1* (ENSG00000172508) were extracted and compared between type I and type II fibre pools within each participant using a Wilcoxon signed rank test.

4.10 | Immunohistochemical detection of CARNS1

Sagittal and frontal cryosections (10 μ m) were cut from whole mouse brains and human white matter samples. Following acetone fixation (10 min) and blocking (30 min, 10% donkey serum in PBS with 1% BSA), sections were exposed overnight at 4°C to antibodies detecting CARNS1 (rabbit polyclonal, 1:100 in PBS with 1% BSA, HPA038569, Sigma). The next day, sections were washed and exposed to complementary secondary antibodies for 60 min (1:500 in PBS with 1% BSA, Thermo Fisher). Fluorescence imaging was performed with a Leica DM4000 B LED (Leica Microsystems). For double-labeling, we used the following antibodies: OLIG2 (1:50, goat polyclonal, AF2418, R&D Systems), neurofilament heavy polypeptide (NF-H, rabbit polyclonal, 1:200, ab8135, Abcam), CD68 (mouse monoclonal, 1:100, M0814 KP1 clone, Dako), and GFAP (mouse monoclonal, 1:100, G3893, Sigma). Absence of CARNS1 from *Carns1*-KO brain sections was used as negative control.

4.11 | Matrix-assisted laser desorption ionization mass spectrometry imaging (MALDI-MSI)

The spatial distribution of carnosine and homocarnosine was studied in mouse brains by MALDI-MSI. Fresh DHB solution (20 mg/mL in 70% MeOH with 0.2% Trifluoroacetic acid) was sprayed using TM-sprayer (HTX Technologies) in a series of 15 layers with the settings: temperature 75°C, pressure 10 psi, flow rate 0.12 mL/min, velocity 1200 mm/min, and track spacing 2 mm. MS acquisition was conducted on a Tims-TOF mass spectrometer (Bruker Daltonik GmbH). The data were acquired at a raster size of 50 \times 50 μ m (or 20 \times 20 μ m for higher spatial resolution) in the mass range of 100–800 m/z in positive ion mode (300 laser shots per pixel with 5000 Hz frequency). After performing the MALDI-MSI experiments, the matrix was gently removed by submersion in EtOH for 2 min. Slides were then washed in serial baths containing 100% EtOH, 90% EtOH, 70% EtOH, or ultrapure water for 3 min each. The sections were stained by hematoxylin for 3 min and eosin for 20 s. Following dehydrating steps, digital images were acquired with the Mirax system (Carl Zeiss) at 40 \times magnification and uploaded on Aperio ImageScope (Leica Biosystems).

4.12 | Statistical analysis

Statistical analyses were performed in GraphPad Prism v9.4 and were described in the appropriate method paragraphs. Significance level was set at $\alpha=0.05$.

ACKNOWLEDGMENTS

For human brain tissues, all material has been collected from donors for or from whom a written informed consent for a brain autopsy and the use of the material and clinical information for research purposes had been obtained by the Netherlands Brain Bank (NBB). The experiment protocols and methods used for analyzing brain samples were conducted with the approval of the NBB and the Medical Ethical Committee of Hasselt University, and carried out according to institutional guidelines. All HCDs analyses were performed using an UHPLC-MS/MS instrument part of the Ghent University MSsmall Expertise Centre for advanced mass spectrometry analysis of small organic molecules. Also, the University Biobank Limburg (UBiLim) is acknowledged for providing storage and release of some human biological material used in this publication. Figure 7D–F, and FG (experimental setups) were created in BioRender. The technical assistance of Jens Jung Nielsen, Anneke Volkaert, Thomas Ehlers, Nicklas Frisch, and Josephine Rol is greatly appreciated.

FUNDING INFORMATION

Research Foundation-Flanders—grant numbers: FWO 11B4220N (TVDS); FWO 1138520N (JS); FWO 11C0421N (SDJ); FWO V433222N (TVDS); FWO G080321N (WD).

CONFLICT OF INTEREST STATEMENT

The authors declare that they have no competing interests.

DATA AVAILABILITY STATEMENT

All data needed to evaluate the conclusions in the paper are present in this article and supplementary materials. Additional data related to this paper can be obtained upon reasonable request to the author.

ORCID

Thibaux Van der Stede  <https://orcid.org/0000-0003-2038-2504>

Jan Spaas  <https://orcid.org/0000-0002-4953-2505>

Sarah de Jager  <https://orcid.org/0000-0002-0447-6888>

Jana De Brandt  <https://orcid.org/0000-0003-3463-1911>

Camilla Hansen  <https://orcid.org/0000-0003-2839-6150>


Jan Stautemas  <https://orcid.org/0000-0001-7473-9340>

Siegrid De Baere  <https://orcid.org/0000-0002-1382-5699>

Siska Croubels  <https://orcid.org/0000-0001-6357-3517>

Michiel Vandenbosch  <https://orcid.org/0000-0002-0427-416X>

Kenneth Verboven  <https://orcid.org/0000-0002-3799-5430>

Dominique Hansen  <https://orcid.org/0000-0003-3074-2737>

Thierry Bové  <https://orcid.org/0000-0003-3786-0699>

Charles Van Praet  <https://orcid.org/0000-0002-4467-0829>

Karel Decaestecker  <https://orcid.org/0000-0003-0767-940X>

Bert O. Eijnde  <https://orcid.org/0000-0002-2262-4661>

Lasse Gliemann  <https://orcid.org/0000-0002-0382-2523>

Ylva Hellsten  <https://orcid.org/0000-0002-2435-9558>

Wim Derave  <https://orcid.org/0000-0002-2225-5587>

reduces methylglyoxal-modified proteins in type-2 diabetic human skeletal muscle cells. *Amino Acids*. 2023;1-8:413-420.

5. Saunders B, Elliott-Sale K, Artioli GG, et al. β -Alanine supplementation to improve exercise capacity and performance: a systematic review and meta-analysis. *Br J Sports Med*. 2017;51(8):658-669.

6. Aldini G, Orioli M, Rossoni G, et al. The carbonyl scavenger carnosine ameliorates dyslipidaemia and renal function in Zucker obese rats. *J Cell Mol Med*. 2011;15(6):1339-1354.

7. Anderson EJ, Vistoli G, Katunga LA, et al. A carnosine analog mitigates metabolic disorders of obesity by reducing carbonyl stress. *J Clin Invest*. 2018;128(12):5280-5293.

8. Spaas J, Franssen W, Keytsman C, et al. Carnosine quenches the reactive carbonyl acrolein in the central nervous system and attenuates autoimmune neuroinflammation. *J Neuroinflammation*. 2021;18(1):1-19.

9. Everaert I, Taes Y, De Heer E, et al. Low plasma carnosinase activity promotes carnosinemia after carnosine ingestion in humans. *Am J Physiol Renal Physiol*. 2012;302:F1537-F1544.

10. Teufel M, Saudek V, Ledig J-P, et al. Sequence identification and characterization of human carnosinase and a closely related non-specific dipeptidase. *J Biol Chem*. 2003;278(8):6521-6531.

11. Drozak J, Veiga-da-Cunha M, Vertommen D, Stroobant V, Van Schaftingen E. Molecular identification of carnosine synthase as ATP-grasp domain-containing protein 1 (ATPGD1). *J Biol Chem*. 2010;285(13):9346-9356.

12. Creighton JV, de Souza GL, Artioli GG, et al. Physiological roles of carnosine in myocardial function and health. *Adv Nutr*. 2022;13(5):1914-1929.

13. Aldini G, Orioli M, Carini M, Maffei FR. Profiling histidine-containing dipeptides in rat tissues by liquid chromatography/electrospray ionization tandem mass spectrometry. *J Mass Spectrom*. 2004;39(12):1417-1428.

14. Wang-Eckhardt L, Bastian A, Bruegmann T, Sasse P, Eckhardt M. Carnosine synthase deficiency is compatible with normal skeletal muscle and olfactory function but causes reduced olfactory sensitivity in aging mice. *J Biol Chem*. 2020;295:17100-17113.

15. Spaas J, Van Noten P, Keytsman C, et al. Carnosine and skeletal muscle dysfunction in a rodent multiple sclerosis model. *Amino Acids*. 2021;53(11):1749-1761.

16. Everaert I, Stegen S, Vanheel B, Taes Y, Derave W. Effect of beta-alanine and carnosine supplementation on muscle contractility in mice. *Med Sci Sports Exerc*. 2013;45(1):43-51.

17. Luo L, Ma W, Liang K, et al. Spatial metabolomics reveals skeletal myofiber subtypes. *Sci Adv*. 2023;9(5):eadd0455.

18. Rubenstein AB, Smith GR, Raue U, et al. Single-cell transcriptional profiles in human skeletal muscle. *Sci Rep*. 2020;10(1):1-15.

19. Nordsborg N, Mohr M, Pedersen LD, Nielsen JJ, Langberg H, Bangsbo J. Muscle interstitial potassium kinetics during intense exhaustive exercise: effect of previous arm exercise. *Am J Physiol Regul Integr Comp Physiol*. 2003;285(1):R143-R148.

20. Reddy A, Bozi LH, Yaghi OK, et al. pH-gated succinate secretion regulates muscle remodeling in response to exercise. *Cell*. 2020;183(1):62-75.e17.

21. Mittenbühler MJ, Jedrychowski MP, Van Vranken JG, et al. Isolation of extracellular fluids reveals novel secreted bioactive proteins from muscle and fat tissues. *Cell Metab*. 2023;35:535-549.e7.

reduces methylglyoxal-modified proteins in type-2 diabetic human skeletal muscle cells. *Amino Acids*. 2023;1-8:413-420.

5. Saunders B, Elliott-Sale K, Artioli GG, et al. β -Alanine supplementation to improve exercise capacity and performance: a systematic review and meta-analysis. *Br J Sports Med*. 2017;51(8):658-669.

6. Aldini G, Orioli M, Rossoni G, et al. The carbonyl scavenger carnosine ameliorates dyslipidaemia and renal function in Zucker obese rats. *J Cell Mol Med*. 2011;15(6):1339-1354.

7. Anderson EJ, Vistoli G, Katunga LA, et al. A carnosine analog mitigates metabolic disorders of obesity by reducing carbonyl stress. *J Clin Invest*. 2018;128(12):5280-5293.

8. Spaas J, Franssen W, Keytsman C, et al. Carnosine quenches the reactive carbonyl acrolein in the central nervous system and attenuates autoimmune neuroinflammation. *J Neuroinflammation*. 2021;18(1):1-19.

9. Everaert I, Taes Y, De Heer E, et al. Low plasma carnosinase activity promotes carnosinemia after carnosine ingestion in humans. *Am J Physiol Renal Physiol*. 2012;302:F1537-F1544.

10. Teufel M, Saudek V, Ledig J-P, et al. Sequence identification and characterization of human carnosinase and a closely related non-specific dipeptidase. *J Biol Chem*. 2003;278(8):6521-6531.

11. Drozak J, Veiga-da-Cunha M, Vertommen D, Stroobant V, Van Schaftingen E. Molecular identification of carnosine synthase as ATP-grasp domain-containing protein 1 (ATPGD1). *J Biol Chem*. 2010;285(13):9346-9356.

12. Creighton JV, de Souza GL, Artioli GG, et al. Physiological roles of carnosine in myocardial function and health. *Adv Nutr*. 2022;13(5):1914-1929.

13. Aldini G, Orioli M, Carini M, Maffei FR. Profiling histidine-containing dipeptides in rat tissues by liquid chromatography/electrospray ionization tandem mass spectrometry. *J Mass Spectrom*. 2004;39(12):1417-1428.

14. Wang-Eckhardt L, Bastian A, Bruegmann T, Sasse P, Eckhardt M. Carnosine synthase deficiency is compatible with normal skeletal muscle and olfactory function but causes reduced olfactory sensitivity in aging mice. *J Biol Chem*. 2020;295:17100-17113.

15. Spaas J, Van Noten P, Keytsman C, et al. Carnosine and skeletal muscle dysfunction in a rodent multiple sclerosis model. *Amino Acids*. 2021;53(11):1749-1761.

16. Everaert I, Stegen S, Vanheel B, Taes Y, Derave W. Effect of beta-alanine and carnosine supplementation on muscle contractility in mice. *Med Sci Sports Exerc*. 2013;45(1):43-51.

17. Luo L, Ma W, Liang K, et al. Spatial metabolomics reveals skeletal myofiber subtypes. *Sci Adv*. 2023;9(5):eadd0455.

18. Rubenstein AB, Smith GR, Raue U, et al. Single-cell transcriptional profiles in human skeletal muscle. *Sci Rep*. 2020;10(1):1-15.

19. Nordsborg N, Mohr M, Pedersen LD, Nielsen JJ, Langberg H, Bangsbo J. Muscle interstitial potassium kinetics during intense exhaustive exercise: effect of previous arm exercise. *Am J Physiol Regul Integr Comp Physiol*. 2003;285(1):R143-R148.

20. Reddy A, Bozi LH, Yaghi OK, et al. pH-gated succinate secretion regulates muscle remodeling in response to exercise. *Cell*. 2020;183(1):62-75.e17.

21. Mittenbühler MJ, Jedrychowski MP, Van Vranken JG, et al. Isolation of extracellular fluids reveals novel secreted bioactive proteins from muscle and fat tissues. *Cell Metab*. 2023;35:535-549.e7.

REFERENCES

- Gulewitsch W, Amiradžibi S. Ueber das Carnosin, eine neue organische Base des Fleischextractes. *Ber Dtsch Chem Ges*. 1900;33(2):1902-1903.
- Boldyrev AA, Aldini G, Derave W. Physiology and pathophysiology of carnosine. *Physiol Rev*. 2013;93(4):1803-1845.
- Aldini G, de Courten B, Regazzoni L, et al. Understanding the antioxidant and carbonyl sequestering activity of carnosine: direct and indirect mechanisms. *Free Radic Res*. 2021;55(4):321-330.
- Matthews JJ, Turner MD, Santos L, Elliott-Sale KJ, Sale C. Carnosine increases insulin-stimulated glucose uptake and

22. Kamal MA, Jiang H, Hu Y, Keep RF, Smith DE. Influence of genetic knockout of Pept2 on the in vivo disposition of endogenous and exogenous carnosine in wild-type and Pept2 null mice. *Am J Physiol Regul Integr Comp Physiol*. 2009;296(4):R986-R991.
23. Peters V, Klessens CQ, Baelde HJ, et al. Intrinsic carnosine metabolism in the human kidney. *Amino Acids*. 2015;47(12):2541-2550.
24. Weigand T, Colbatzky F, Pfeffer T, et al. A global Cndp1-knockout selectively increases renal carnosine and anserine concentrations in an age- and gender-specific manner in mice. *Int J Mol Sci*. 2020;21(14):4887.
25. Heidenreich E, Pfeffer T, Kracke T, et al. A novel UPLC-MS/MS method identifies organ-specific dipeptide profiles. *Int J Mol Sci*. 2021;22(18):9979.
26. Abraham D, Pisano JJ, Udenfriend S. The distribution of homocarnosine in mammals. *Arch Biochem Biophys*. 1962;99(2):210-213.
27. Kish SJ, Perry TL, Hansen S. Regional distribution of homocarnosine, homocarnosine-carnosine synthetase and homocarnosinase in human brain. *J Neurochem*. 1979;32(6):1629-1636.
28. Derave W, Everaert I, Beeckman S, Baguet A. Muscle carnosine metabolism and β -alanine supplementation in relation to exercise and training. *Sports Med*. 2010;40(3):247-263.
29. Mannion A, Jakeman P, Dunnett M, Harris R, Willan P. Carnosine and anserine concentrations in the quadriceps femoris muscle of healthy humans. *Eur J Appl Physiol Occup Physiol*. 1992;64(1):47-50.
30. C. Harris R, Dunnett M, Greenhaff PL. Carnosine and taurine contents in individual fibres of human vastus lateralis muscle. *J Sports Sci*. 1998;16(7):639-643.
31. Baguet A, Everaert I, De Naeyer H, et al. Effects of sprint training combined with vegetarian or mixed diet on muscle carnosine content and buffering capacity. *Eur J Appl Physiol*. 2011;111(10):2571-2580.
32. Margolis FL. Carnosine in the primary olfactory pathway. *Science*. 1974;184(4139):909-911.
33. Mahootchi E, Cannon Homaei S, Kleppe R, et al. GADL1 is a multifunctional decarboxylase with tissue-specific roles in β -alanine and carnosine production. *Sci Adv*. 2020;6(29):eabb3713.
34. Zhang Y, Chen K, Sloan SA, et al. An RNA-sequencing transcriptome and splicing database of glia, neurons, and vascular cells of the cerebral cortex. *J Neurosci*. 2014;34(36):11929-11947.
35. Consortium TM, GROUP STW. Single-cell transcriptomics of 20 mouse organs creates a Tabula Muris. *Nature*. 2018;562(7727):367-372.
36. O'Dowd JJ, Robins DJ, Miller DJ. Detection, characterisation, and quantification of carnosine and other histidyl derivatives in cardiac and skeletal muscle. *Biochim Biophys Acta*. 1988;967(2):241-249.
37. Johnson P, Hammer JL. Histidine dipeptide levels in ageing and hypertensive rat skeletal and cardiac muscles. *Comp Biochem Physiol B*. 1992;103(4):981-984.
38. Flancbaum L, Fitzpatrick J, Brotman D, Marcoux A-M, Kasziba E, Fisher H. The presence and significance of carnosine in histamine-containing tissues of several mammalian species. *Agents Actions*. 1990;31:190-196.
39. Liu Y, Su D, Zhang L, et al. Endogenous L-carnosine level in diabetes rat cardiac muscle. *Evid Based Complement Alternat Med*. 2016;2016:6230825.
40. Chan WK, Decker EA, Chow CK, Boissonneault GA. Effect of dietary carnosine on plasma and tissue antioxidant concentrations and on lipid oxidation in rat skeletal muscle. *Lipids*. 1994;29(7):461-466.
41. Li VL, He Y, Contrepois K, et al. An exercise-inducible metabolite that suppresses feeding and obesity. *Nature*. 2022;606(7915):785-790.
42. Kim JT, Li VL, Terrell SM, Fischer CR, Long JZ. Family-wide annotation of enzymatic pathways by parallel in vivo metabolomics. *Cell Chem Biol*. 2019;26(11):1623-9.e3.
43. Yan K, Mei Z, Zhao J, et al. Integrated multilayer omics reveals the genomic, proteomic, and metabolic influences of Histidyl dipeptides on the heart. *J Am Heart Assoc*. 2022;11(13):e023868.
44. Zhao J, Conklin DJ, Guo Y, et al. Cardiospecific overexpression of ATPGD1 (carnosine synthase) increases histidine dipeptide levels and prevents myocardial ischemia reperfusion injury. *J Am Heart Assoc*. 2020;9:e015222.
45. de Souza GL, Sales LP, Saito TR, et al. Histidine dipeptides are key regulators of excitation-contraction coupling in cardiac muscle: evidence from a novel CARNS1 knockout rat model. *Redox Biol*. 2021;44:102016.
46. Swietach P, Youm J-B, Saegusa N, Leem C-H, Spitzer KW, Vaughan-Jones RD. Coupled $\text{Ca}^{2+}/\text{H}^{+}$ transport by cytoplasmic buffers regulates local Ca^{2+} and H^{+} ion signaling. *Proc Natl Acad Sci USA*. 2013;110(22):E2064-E2073.
47. Swietach P, Leem CH, Spitzer KW, Vaughan-Jones RD. Pumping Ca^{2+} up H^{+} gradients: a $\text{Ca}^{2+}-\text{H}^{+}$ exchanger without a membrane. *J Physiol*. 2014;592(15):3179-3188.
48. Gardner M, Illingworth KM, Kelleher J, Wood D. Intestinal absorption of the intact peptide carnosine in man, and comparison with intestinal permeability to lactulose. *J Physiol*. 1991;439(1):411-422.
49. Harris RC, Tallon M, Dunnett M, et al. The absorption of orally supplied β -alanine and its effect on muscle carnosine synthesis in human vastus lateralis. *Amino Acids*. 2006;30(3):279-289.
50. Baguet A, Everaert I, Yard B, et al. Does low serum carnosinase activity favour high-intensity exercise capacity? *Am J Physiol Heart Circ Physiol*. 2014;116:553-559.
51. Pandya VK, Sonwane B, Rathore R, Unnikrishnan A, Kumaran S, Kulkarni MJ. Development of multiple reaction monitoring assay for quantification of carnosine in human plasma. *RSC Adv*. 2020;10(2):763-769.
52. de Jager S, Blancquaert L, Van der Stede T, et al. The ergogenic effect of acute carnosine and anserine supplementation: dosing, timing, and underlying mechanism. *J Int Soc Sports Nutr*. 2022;19(1):70-91.
53. Pegova A, Abe H, Boldyrev A. Hydrolysis of carnosine and related compounds by mammalian carnosinases. *Comp Biochem Physiol B, Biochem Mol Biol*. 2000;127(4):443-446.
54. Oppermann H, Elsel S, Birkemeyer C, Meixensberger J, Gaunitz F. Erythrocytes prevent degradation of carnosine by human serum carnosinase. *Int J Mol Sci*. 2021;22(23):12802.
55. Posa DK, Miller J, Hoetker D, et al. Skeletal muscle analysis of cancer patients reveals a potential role for carnosine in muscle wasting. *J Cachexia Sarcopenia Muscle*. 2023. [Online ahead of print]. doi:10.1002/jcsm.13258

56. Nagai K, Nijijima A, Yamano T, et al. Possible role of L-carnosine in the regulation of blood glucose through controlling autonomic nerves. *Exp Biol Med*. 2003;228(10):1138-1145.
57. Severinsen MCK, Pedersen BK. Muscle–organ crosstalk: the emerging roles of myokines. *Endocr Rev*. 2020;41(4):594-609.
58. Pedersen BK, Febbraio MA. Muscles, exercise and obesity: skeletal muscle as a secretory organ. *Nat Rev Endocrinol*. 2012;8(8):457-465.
59. Murphy RM, Watt MJ, Febbraio MA. Metabolic communication during exercise. *Nat Metab*. 2020;2(9):805-816.
60. Park G, Haley JA, Le J, et al. Quantitative analysis of metabolic fluxes in brown fat and skeletal muscle during thermogenesis. *Nat Metab*. 2023. [Online ahead of print]. doi:[10.1038/s42255-023-00825-8](https://doi.org/10.1038/s42255-023-00825-8)
61. Nelson ME, Madsen S, Cooke KC, et al. Systems-level analysis of insulin action in mouse strains provides insight into tissue- and pathway-specific interactions that drive insulin resistance. *Cell Metab*. 2022;34(2):227-39.e6.
62. Ihara H, Kakihana Y, Yamakage A, et al. 2-Oxo-histidine-containing dipeptides are functional oxidation products. *J Biol Chem*. 2019;294(4):1279-1289.
63. Baba SP, Hoetker JD, Merchant M, et al. Role of aldose reductase in the metabolism and detoxification of carnosine-acrolein conjugates. *J Biol Chem*. 2013;288(39):28163-28179.
64. Carvalho VH, Oliveira AH, de Oliveira LF, et al. Exercise and β -alanine supplementation on carnosine-acrolein adduct in skeletal muscle. *Redox Biol*. 2018;18:222-228.
65. Wang-Eckhardt L, Becker I, Wang Y, Yuan J, Eckhardt M. Absence of endogenous carnosine synthesis does not increase protein carbonylation and advanced lipoxidation end products in brain, kidney or muscle. *Amino Acids*. 2022;54:1013-1023.
66. Van der Stede T, Blancquaert L, Stassen F, et al. Histamine H1 and H2 receptors are essential transducers of the integrative exercise training response in humans. *Sci Adv*. 2021;7(16):eabf2856.
67. Verboven K, Wouters K, Gaens K, et al. Abdominal subcutaneous and visceral adipocyte size, lipolysis and inflammation relate to insulin resistance in male obese humans. *Sci Rep*. 2018;8(1):1-8.
68. Van de Velde F, Ouwens DM, Batens A-H, Van Nieuwenhove Y, Lapauw B. Divergent dynamics in systemic and tissue-specific metabolic and inflammatory responses during weight loss in subjects with obesity. *Cytokine*. 2021;144:155587.
69. Chaleckis R, Murakami I, Takada J, Kondoh H, Yanagida M. Individual variability in human blood metabolites identifies age-related differences. *Proc Natl Acad Sci USA*. 2016;113(16):4252-4259.
70. De Brandt J, Derave W, Vandenabeele F, et al. Efficacy of 12 weeks oral beta-alanine supplementation in patients with chronic obstructive pulmonary disease: a double-blind, randomized, placebo-controlled trial. *J Cachexia Sarcopenia Muscle*. 2022;13(5):2361-2372.
71. Gliemann L, Rytter N, Piil P, et al. The endothelial mechanotransduction protein platelet endothelial cell adhesion molecule-1 is influenced by aging and exercise training in human skeletal muscle. *Front Physiol*. 2018;9:1807.
72. Gliemann L, Rytter N, Tamariz-Elleemann A, et al. Lifelong physical activity determines vascular function in late postmenopausal women. *Med Sci Sports Exerc*. 2020;52(3):627-636.
73. Olsen L, Hoier B, Hansen C, et al. Angiogenic potential is reduced in skeletal muscle of aged women. *J Physiol*. 2020;598(22):5149-5164.
74. Hansen C, Møller S, Ehlers T, et al. Redox balance in human skeletal muscle-derived endothelial cells-effect of exercise training. *Free Radic Biol Med*. 2022;179:144-155.
75. Hoier B, Olsen K, Nyberg M, Bangsbo J, Hellsten Y. Contraction-induced secretion of VEGF from skeletal muscle cells is mediated by adenosine. *Am J Physiol Heart Circ Physiol*. 2010;299(3):H857-H862.
76. Perry CG, Kane DA, Lin C-T, et al. Inhibiting myosin-ATPase reveals a dynamic range of mitochondrial respiratory control in skeletal muscle. *Biochem J*. 2011;437(2):215-222.
77. de Jager S, Van Damme S, De Baere S, et al. No effect of acute Balenine supplementation on maximal and submaximal exercise performance in recreational cyclists. *Int J Sport Nutr Exerc Metab*. 2023;33(2):84-92.
78. de Jager S, Vermeulen A, De Baere S, et al. Acute balenine supplementation in humans as a natural carnosinase-resistant alternative to carnosine. *Sci Rep*. 2023;13(1):6484.
79. Larsen MR, Steenberg DE, Birk JB, et al. The insulin-sensitizing effect of a single exercise bout is similar in type I and type II human muscle fibres. *J Physiol*. 2020;598(24):5687-5699.
80. Love MI, Huber W, Anders S. Moderated estimation of fold change and dispersion for RNA-seq data with DESeq2. *Genome Biol*. 2014;15(12):1-21.

SUPPORTING INFORMATION

Additional supporting information can be found online in the Supporting Information section at the end of this article.

How to cite this article: Van der Stede T, Spaas J, de Jager S, et al. Extensive profiling of histidine-containing dipeptides reveals species- and tissue-specific distribution and metabolism in mice, rats, and humans. *Acta Physiol*. 2023;239:e14020. doi:[10.1111/apha.14020](https://doi.org/10.1111/apha.14020)